The Supermassive Black Hole at the Galactic Center

Fulvio Melia[1]
Physics Department and Steward Observatory, The University of Arizona, Tucson, AZ 85721

Heino Falcke

Max-Planck-Institut für Radioastronomie, Auf dem Hügel 69, Bonn D-53121, Germany

KEYWORDS: accretion, black hole physics, gas dynamics, jets, magnetohydrodynamics, radio synchrotron, radio polarization, stellar kinematics

ABSTRACT: The inner few parsecs at the Galactic Center have come under intense scrutiny in recent years, in part due to the exciting broad-band observations of this region, but also because of the growing interest from theorists motivated to study the physics of black hole accretion, magnetized gas dynamics and unusual star formation. The Galactic Center is now known to contain arguably the most compelling supermassive black hole candidate, weighing in at a little over 2.6 million suns. Its interaction with the nearby environment, comprised of clusters of evolved and young stars, a molecular dusty ring, ionized gas streamers, diffuse hot gas, and a hypernova remnant, is providing a wealth of accretion phenomenology and high-energy processes for detailed modeling. In this review, we summarize the latest observational results, and focus on the physical interpretation of the most intriguing object in this region—the compact radio source Sgr A*, thought to be the radiative manifestation of the supermassive black hole.

to appear in: Annual Review of Astronomy & Astrophysics, Vol. 39 (2001)

CONTENTS

INTRODUCTION 2

THE GALACTIC CENTER COMPONENTS 3

PHENOMENOLOGY OF SGR A* 7
*The Discovery of Sgr A** 7
The Concentration of Dark Matter 8
*Position and Proper Motion of Sgr A** 9
Size Constraints and the Brightness Temperature 11
*The Spectrum of Sgr A** 13
*Radio Variability of Sgr A** 15
*The Measured Linear Polarization of Sgr A** 15
*The Measured Circular Polarization of Sgr A** 17

GAS DYNAMICS AND STELLAR WIND CAPTURE 18

[1]Sir Thomas Lyle Fellow and Miegunyah Fellow.

EMISSION MODELS FOR SGR A* 22
Emission due to the Accreting Plasma 22
Emission due to Non-Accretion Processes 28
Alternatives to the Black Hole Paradigm 32

STRONG GRAVITY EFFECTS 33
Imaging the Event Horizon 33
Interactions of Sgr A with the Central Star Cluster* 35

SGR A* AS A MODEL FOR AGN ACTIVITY 36

CONCLUSIONS 38

1 INTRODUCTION

The region bounded by the inner few parsecs at the Galactic Center contains six principal components that coexist within the central deep gravitational potential well of the Milky Way. These constituents are a supermassive black hole, the surrounding cluster of evolved and young stars, a molecular dusty ring, ionized gas streamers, diffuse hot gas, and a powerful supernova-like remnant. Many of the observed phenomena occurring in this complex and unique portion of the Galaxy can be explained by the interaction of these components.

Though largely shrouded by the intervening gas and dust, the Galactic Center is now actively being explored observationally at radio, sub-millimeter, infrared, X-ray and γ-ray wavelengths with unprecedented clarity and spectral resolution. The interactions governing the behavior and evolution of this nucleus are attracting many astronomers and astrophysicists interested in learning about the physics of black hole accretion, magnetized gas dynamics and unusual stellar formation, among others. The Galactic Center is one of the most interesting regions for scientific investigation because it is the closest available galactic nucleus and therefore can be studied with a resolution that is impossible to achieve in other galaxies. One arcsecond at the Galactic Center distance of ~ 8 kpc corresponds to only 0.04 pc ($\approx 1.2 \times 10^{17}$ cm. Thus, developing a consistent theoretical picture of the phenomena we observe there improves not only our understanding of the Galaxy, but also our view of galactic nuclei in general.

For example, the Galactic Center is now known to harbor by far the most evident condensation of dark mass, which is apparently coincident with the compact radio source Sgr A*, the primary subject of this review. An overwhelming number of observations (proper and radial motion of stars and gas) now strongly supports the idea that this compact radio source in the center of the Galaxy has a mass of $2.6 \times 10^6\ M_\odot$ (see § 3.2). Because of these unique observations and the proximity of Sgr A*, the supermassive black hole paradigm for galactic cores may be strengthened or refuted based on what we learn about the Galactic Center.

The properties of Sgr A* are, of course, not independent of its environment. For example, one might naively expect from the observed nearby gas dynamics, that Sgr A* should be a bright source. Yet it is underluminous at all wavelengths by many orders of magnitude, radiating at only 3×10^{-10} of its Eddington luminosity. Does this imply new accretion physics (as has been proposed) or does it imply something peculiar about Sgr A* itself? What now makes asking these questions meaningful is that the extensive sets of data seriously constrain the currently proposed answers.

Over the past decade the number of papers appearing in refereed journals dealing with the theory of phenomena in the Galactic Center, particularly the physics of Sgr A*, has doubled roughly every three years. The rate at which papers on the Galactic Center appear is now more than one per week. It is our intention here to summarize the principal observational constraints, and to focus on the key theoretical questions now facing the growing number of astrophysicists working in this field.

2 THE GALACTIC CENTER COMPONENTS

It is thought that the dynamical center of the Galaxy coincides with Sgr A* (Eckart et al. 1995; Menten et al. 1997; Ghez et al. 1998), a compact non-thermal radio source no bigger than ~ 1 AU (see § 3; Krichbaum et al. 1993; Backer et al. 1993; Lo et al. 1993; Rogers et al. 1994; Krichbaum et al. 1998; Lo et al. 1998). On a slightly larger scale, the "three-arm" spiral configuration of ionized gas and dust known as Sgr A West (Ekers et al. 1983; Lo & Claussen 1983) engulfs this source in projection (Fig. 1; here shown in a ~ 2 pc $\times$ 2 pc image). Figure 2 shows the stellar distribution at 1.6μm (on roughly the same spatial scale as Fig. 1) as seen by NICMOS on the Hubble Space Telescope *HST*. Sgr A* is in the very middle of this field of view, though it is not seen at this wavelength.

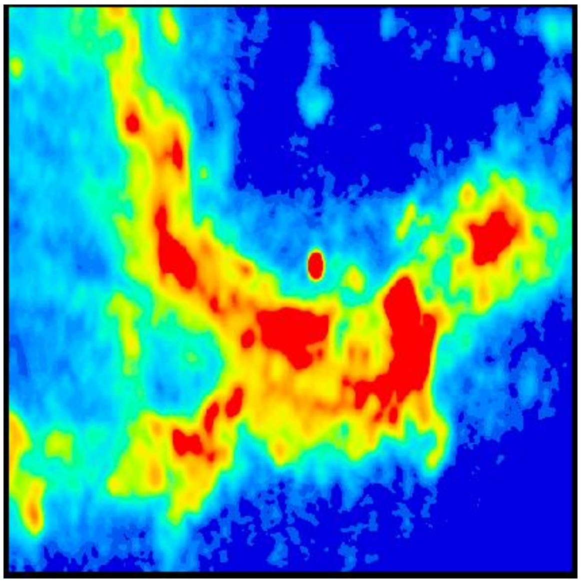

Figure 1 Sub-arcsec (2 cm) image of Sgr A West and Sgr A*. The cometary-like feature to the north of Sgr A* (identified as the bright central spot in this image) is associated with the luminous star IRS 7, seen at the corresponding location in Fig. 2. (From Yusef-Zadeh & Wardle 1993.)

Sgr A West probably derives its heat from the central distribution of bright stars, rather than from a single point source (such as Sgr A*; Zylka et al. 1995; Gezari 1996; Chan et al. 1997; Latvakoski et al. 1999). Some hot and luminous stars are thought to have been formed as recently as a few million years ago (Tamblyn & Rieke 1993; Najarro et al. 1994; Krabbe et al. 1995; Figer et al.

1999a). We therefore see a sprinkling of several infrared-bright sources throughout Sgr A West that are probably embedded luminous stars, some of which may be extended (Gezari 1996; Tanner et al. 1999). It is not yet clear whether these particular stars have formed within the streamer or just happen to lie along the line of sight (see Fig. 2).

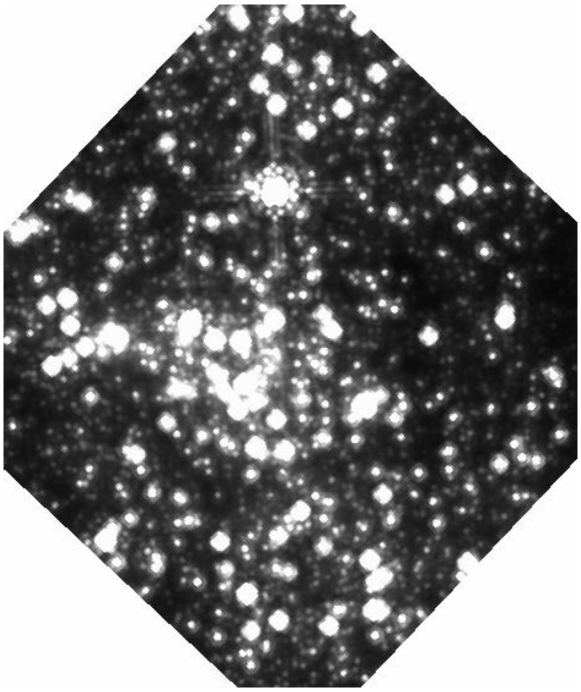

Figure 2 NICMOS 1.6μm image of the inner $19'' \times 19''$ region at the Galactic Center. This is the same field as that shown in Fig. 1. (Image courtesy of M. Rieke, Steward Observatory.)

Spectroscopy of the hot gas in the mini-spiral structure seen in Figure 1 (Serabyn et al. 1988; Herbst et al. 1993; Roberts, Yusef-Zadeh, & Goss 1996) suggests that it is rotating with a velocity of about 150 km s^{-1} around Sgr A* in a counter-clock wise direction; this confirms the inference drawn from the Very Large Array (VLA) proper motion studies (Yusef-Zadeh, Roberts, & Biretta 1998; Zhao & Goss 1998; Zhao & Goss 1999), which have in addition shown the presence of high-velocity features—such as the "bullet" (see Fig. 3)—between 400 and 1,200 km s^{-1}. The stream is evidently tugging along a milli-Gauss magnetic field seen through MIR polarization imaging (Aitken et al. 1991; Aitken et al. 1998) with projected field lines aligned with the flow.

One of the most striking structures in Sgr A West is the "minicavity" centered near the junction of its northern and eastern arms. This feature, adjacent to the peculiar sources Sgr A* and IRS16 (the bright blue stellar cluster to the east of Sgr A*), is a distinct hole in the distribution of the radio continuum emission (Fig. 1) and the Pa α emission (Fig. 3) with a diameter of $2''$, corresponding to a linear dimension of 0.08 pc. It may have been created by a spherical wind, the

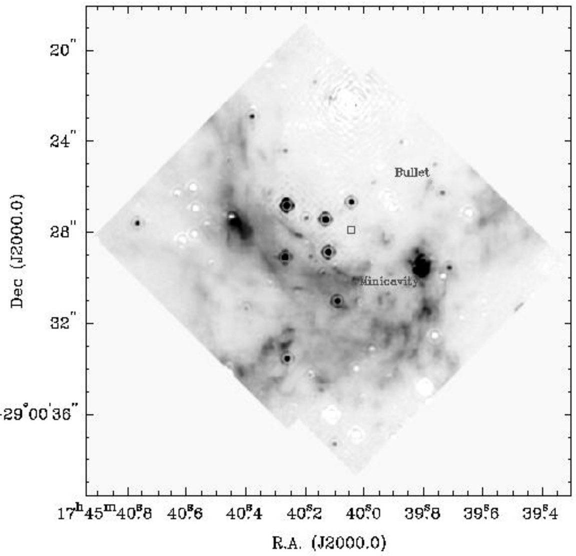

Figure 3 Pa α mosaic of the central parsec (logarithmic inverse gray scale with a dynamic range of 100) with $0\farcs2$ resolution. Note the wispy, filamentary structure in the ionized gas and the sharp-edged bubble to the lower right known as the "minicavity". The fast-moving "bullet" is also shown (the label is northeast of the feature). A box centered on Sgr A* is shown for reference. Some stars are also visible. (From Stolovy et al. 1999.)

source of which is yet to be identified, or it may be due in part to the effects of a focused gas flow from the direction of Sgr A* (Melia, Coker, & Yusef-Zadeh 1996).

On an even larger scale (~ 3 pc), Sgr A West is thought to lie within a large central cavity that is surrounded by a gaseous circumnuclear ring (or circumnuclear disk, CND; Becklin, Gatley, & Werner 1982; Davidson et al. 1992; Latvakoski et al. 1999; Zylka et al. 1999) and is otherwise relatively devoid of neutral gas, with the possible exception of a "tongue" of atomic gas that appears to be falling in from the north (Jackson et al. 1993). A superposition of the radio continuum emission from Sgr A West due to free-free radiation with an image showing the distribution of molecular gas (Fig. 4) suggests that this central cavity is filled with a bath of ultraviolet radiation heating the dust and gas within the inner 8 pc of the galaxy (Yusef-Zadeh et al. 1999).

Radio continuum measurements of the larger-scale (~ 50 pc $\times$ 50 pc) distribution of hot gas, known as the Sgr A complex, show a rather complicated morphology. Recent improvements in spatial resolution and large scale imaging with the VLA have helped considerably in separating the thermal and non-thermal features in this region (Ekers et al. 1983; Yusef-Zadeh & Morris 1987; Pedlar et al. 1989). Sgr A West and Sgr A East constitute the brightest of the continuum features (see Fig. 5). Sgr A East could be a supernova remnant (perhaps a bubble driven by several supernovae) or a very low-luminosity example of a radio component associated with the active nucleus of a spiral galaxy (Pedlar et al. 1989). Observations of Sgr A East show it to be associated with the prominent 50 km s^{-1} molecular cloud near the Galactic Center. Such an association would require more than 10^{52} erg of explosive energy to account for the origin of Sgr A East (Mezger et al. 1989), making it rather a hypernova remnant—perhaps due

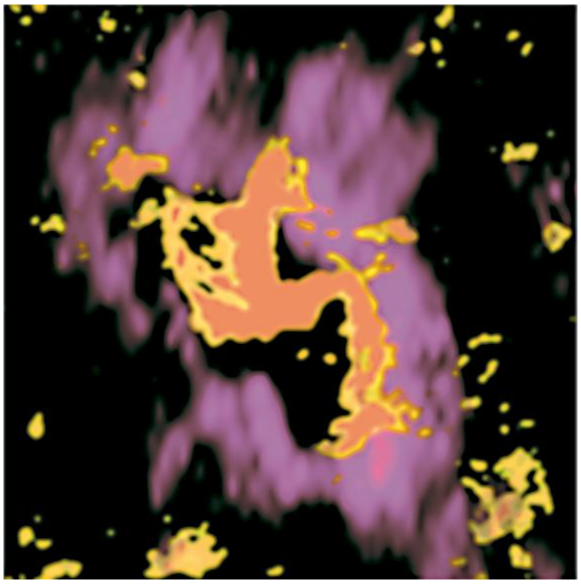

Figure 4 A radio image of ionized gas (Sgr A West) at $\lambda = 1.2$cm with its three-arm appearance, shown in orange, superimposed on the distribution of HCN emission, displayed in red (Wright et al. 1993). Most of the ionized gas is distributed in the molecular cavity. At the distance to the Galactic Center, this image corresponds to a size of approximately 4 pc on each side. (From Yusef-Zadeh, Melia, & Wardle 2000.)

to a tidally disrupted star (Khokhlov & Melia 1996). On the other hand, recent X-ray observations (Maeda et al. 2001) may favor a classification as a young ($\sim 10^4$ yr) metal-rich mixed-morphology supernova remnant.

The Sgr A complex is also associated with diffuse X-ray emission (Predehl & Trümper 1994; Koyama et al. 1996; Sidoli & Mereghetti 1999; Baganoff et al. 2001). The large temperature and pressure of the emitting region producing the hard X-rays suggest that this gas is probably unbound. The size of this feature, and its sound speed, argue for an age of $\sim$50,000 years for the hot plasma bubble (Koyama et al. 1996).

On a scale of hundreds of parsecs, several synchrotron-emitting filamentary structures run roughly in the direction perpendicular to the Galactic plane (Yusef-Zadeh, Morris, & Chance 1984; Liszt 1985; Bally & Yusef-Zadeh 1989; Gray et al. 1991; Lang, Morris, & Echevarria 1999; Reich, Sofue, & Matsuo 2000). These filaments are possibly magnetic field lines (pervading the Galaxy) that are lit up by relativistic electrons, e.g., in a reconnection zone between the Galactic field lines and those from molecular clouds, injected with ionized particles from a hot star cluster (Serabyn & Morris 1994; Figer et al. 1999b).

The geometry of the Galactic magnetic field is generally thought to be poloidal within ~ 100 pc of the nucleus (Morris 1994; Sofue & Lang 1999) with a milli-Gauss intensity (Killeen, Lo, & Crutcher 1992; Plante, Lo, & Crutcher 1995; Roberts 1999). The field lines also appear to be stretched in the azimuthal direction within molecular clouds (Novak 1999; Novak et al. 2000).

The morphology of the large scale region at the Galactic Center is very rich. More detailed accounts of these observations are provided in the reviews by Morris & Serabyn (1996) and Mezger, Duschl, & Zylka (1996). A beautiful (and detailed) large-scale view of the Galactic Center at 90 cm wavelength is presented by

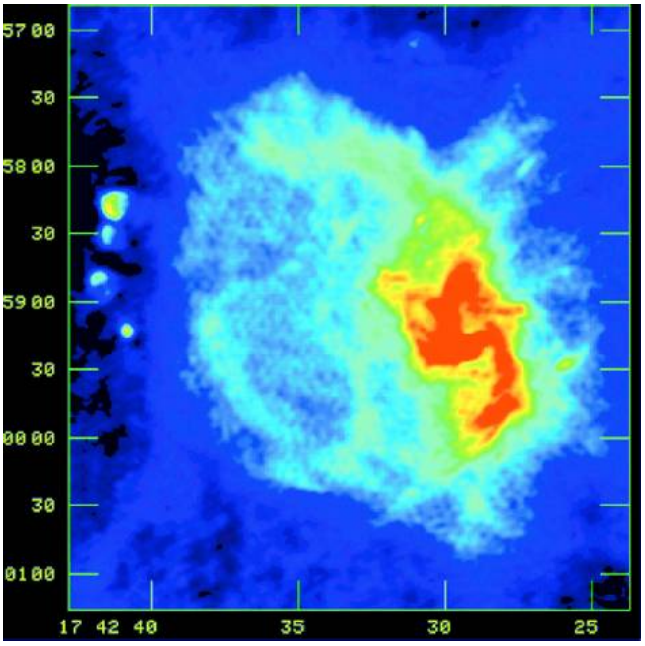

Figure 5 VLA radio continuum image of the Galactic Center showing the shell-like structure of the non-thermal Sgr A East (light blue and green) and the spiral-shaped structure of the thermal Sgr A West (red) at $\lambda = 6$cm with a resolution of $3.4'' \times 2.9''$. A cluster of HII regions associated with Sgr A East is also evident to the east of the shell. The weak extended features (dark blue) surrounding the shell are part of the Sgr A East halo. (From Yusef-Zadeh, Melia, & Wardle 2000.)

LaRosa et al. (2000). Below, we shall concentrate on the phenomenology and theory of the most enigmatic object within this array of sources at the Galactic Center—the supermassive black hole candidate, Sgr A*.

3 PHENOMENOLOGY OF SGR A*

*3.1 The Discovery of Sgr A**

The prescient application of the then very speculative black hole model for quasars led Lynden-Bell & Rees (1971) to point out that the Galactic Center also should contain a supermassive black hole, perhaps detectable with radio interferometry. Subsequently, Balick & Brown (1974) indeed found a compact radio source with the National Radio Astronomy Observatory (NRAO) interferometer at Green Bank, later to be confirmed by Westerbork (Ekers et al. 1975) and Very Large Baseline Interferometry (VLBI) observations (Lo et al. 1975). Eight years after its discovery, the unresolved source was named Sgr A* by Brown (1982) to distinguish it from the more extended emission of the Sgr A complex, and to emphasize its uniqueness. More precise high-resolution Very Large Array (VLA) observations (Brown, Johnston, & Lo 1981) indicated that it was located near the dynamical center of the gas streamers in the Galactic nucleus, as inferred from infrared fine-structure lines (Ne II; Lacy et al. 1980). Its radio variability was established at about this time (Brown & Lo 1982). The accumulation of these observational signatures make it clear that Sgr A* is a very unusual object, rendering it a prime suspect for the location of the putative supermassive black hole.

3.2 The Concentration of Dark Matter

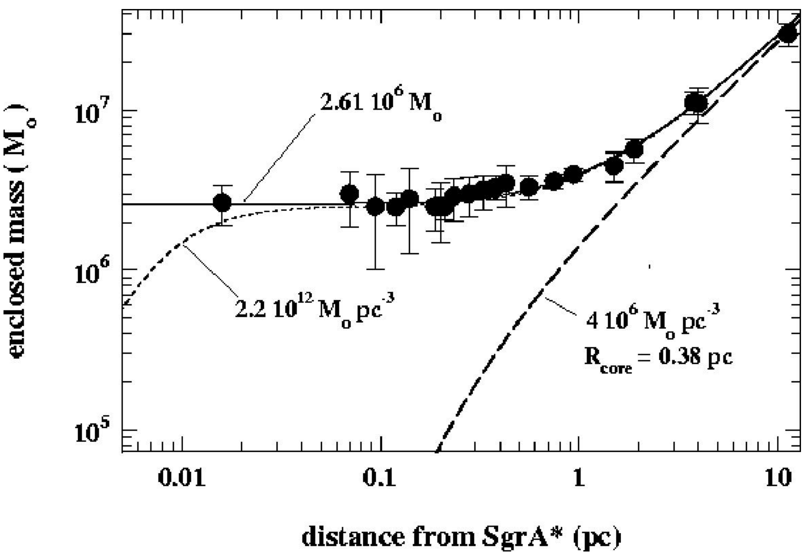

Figure 6 A plot of the distribution of enclosed mass versus distance from Sgr A*. The three curves represent the mass model for a nearly isothermal stellar cluster with a core radius of 0.38 pc (thick dashed line), the sum of this cluster plus a point mass of $2.61 \pm 0.35 \times 10^6$ $M_\odot$ (thin solid curve), the same cluster and a dark cluster with a central density of 2.2×10^{12} $M_\odot$ pc^{-3} and a core radius of 0.0065 pc (thin dotted curve). (From Genzel & Eckart 1999.)

In their review, Genzel & Townes (1987) published the now well-known diagram showing the enclosed mass versus distance from Sgr A*, suggesting a concentration of matter with a point-like object (of mass $\sim 3 \times 10^6 M_\odot$) at the Galactic Center. This estimate depended rather sensitively on the mass inferred from the ionized gas motions (Serabyn & Lacy 1985; Serabyn et al. 1988), which some thought could have been influenced by non-gravitational forces (e.g., magnetic fields, stellar winds, etc.). Even so, it was difficult to see how the observed stellar winds and the measured magnetic fields in this general region could be strong enough to produce the observed velocities. In addition, infall from a large distance would have difficulty accounting for the patterns seen (Townes 1996). The evidence for the existence of a dark mass concentration has significantly and steadily grown since then—mainly via infra-red observations of stars near Sgr A*.

The distribution of stellar radial velocities was inferred from spectroscopic measurements, first for late-type giants and AGB stars (Rieke & Rieke 1988; Sellgren et al. 1990) and later for the hot "He II-stars"—blue supergiants close to their Wolf-Rayet stage (Najarro et al. 1997)—down to a distance of $1''$ from Sgr A* (Krabbe et al. 1995; Haller et al. 1996; Genzel et al. 1996). The most recent breakthrough has been provided by near-infrared speckle imaging methods (i.e., shift-and-add techniques) that facilitated the creation of a remarkable set of stellar proper motion data acquired over a six year-period with the ESO NTT, and later with Keck (Eckart & Genzel 1996; Eckart & Genzel 1997; Ghez et al. 1998).

These measurements trace the stellar trajectories down to a scale as small as 5 light days from Sgr A*.

The suggested central dark mass within the inner 0.015 pc of the Galactic Center is $2.61 \pm 0.35 \times 10^6\ M_\odot$. ($0''.1$ corresponds to 800 Astronomical Units, or roughly 1.2×10^{16} cm at a distance of 8 kpc.) The inferred distribution of matter as a function of distance from Sgr A* is shown in Figure 6, and the measured stellar velocity dispersion (shown in the accompanying Fig. 7) is fully consistent with Keplerian motion about a highly compact central mass concentration. The value of these observations cannot be overstated, since they establish the presence of a dark mass in the Galactic Center beyond a reasonable doubt, even though several systematic uncertainties (on a 10% level) still remain; these include the exact distance to the Galactic Center ($\sim$ 8 kpc; see Reid 1993) and the exact mass estimator used to convert velocities to masses. The characteristic size associated with such a mass is the Schwarzschild radius $r_s \equiv 2GM/c^2$, which is here equal to 7.7×10^{11} cm. At a distance of 8 kpc, this corresponds to $6.4\,\mu$as.

However, showing that the Galactic Center must contain a centralized mass concentration does not yet necessarily imply that this dark matter is in the form of an ultra-compact object with a few million solar masses. Nor does it exclusively imply that the unusual radio source Sgr A* must be associated with it; but it is possible to demonstrate that Sgr A* is not star-like, based on its position and proper motion, which we consider next.

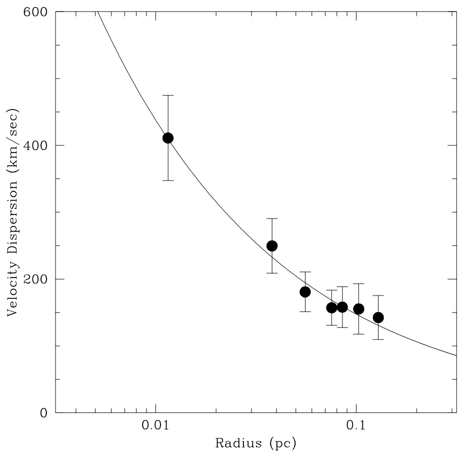

Figure 7 The projected stellar velocity dispersion versus the distance from Sgr A*. The solid curve represents Keplerian motion due to a mass concentrated within 0.01 pc. These data were obtained with the Keck telescope. (From Ghez et al. 1999.)

*3.3 Position and Proper Motion of Sgr A**

To begin with, how well does Sgr A* actually coincide with the dynamical center of the stellar cluster? Thanks to the pioneering work of Menten et al. (1997), who found an SiO maser in the bright star IRS 7 with the VLA, the location of Sgr A* in the near-infrared frame is now known to within 30 mas. Source counts (Eckart et al. 1993) of the Near Infrared (NIR) stars show the center of the distribution coincides with Sgr A* to within fractions of an arcsecond. Similarly, using an unbiased approach to identify stellar proper motions, Ghez et al. (1998) find that the gravitational potential peaks on Sgr A* within $\sim 0.''1$. Recently, Ghez et al. (2000) announced the detection of the first signs of acceleration in the motion of stars allowing one to calculate their orbits. The first results indicate that the dynamical center of these bound trajectories coincides with Sgr A* to within about 50 mas (Fig. 8). Another interesting by-product of these measurements is that the assumption of Keplerian motion may also help us to determine the distance to the Galactic Center more precisely (Salim & Gould 1999).

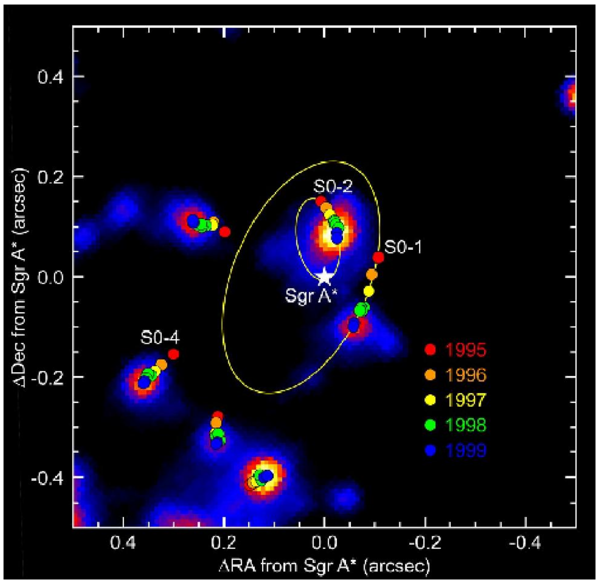

Figure 8 The orbits of two stars (labeled S0-1 and S0-2) around Sgr A* as inferred from the detection of acceleration in their proper motion. The individual positions at the various epochs are shown as colored dots. The underlying image is a K-band Keck telescope image of the stars in the Galactic Center. (From Ghez et al. 2000)

Of equal significance is the argument first advanced by Backer (1996), that a heavy object in dynamical equilibrium with the surrounding stellar cluster will move slowly, so that a failure to detect random proper motion in Sgr A* may be used as a balance with which to weigh it. In fact, such measurements have been carried out using the VLA (for about 16 years; Backer & Sramek 1999) and the VLBA (Reid et al. 1999), yielding consistent results of a similar quality. For example, the latter yield a proper motion in Sgr A* of -3.33 ± 0.1 E and -4.94 ± 0.4 N mas yr^{-1}, which corresponds to -5.90 ± 0.35 and $+0.20 \pm 0.30$ mas yr^{-1} in Galactic longitude and latitude, respectively. This apparent motion amounts to a constant velocity that is entirely consistent with the 220 km s^{-1} rotation of our solar system around the Galactic Center. The position of Sgr A* at 1996.25 in J2000 coordinates was

$$\mathrm{RA}(1996.25) = 17^{\mathrm{h}}45^{\mathrm{m}}40.^{\mathrm{s}}0409, \quad \mathrm{DEC}(1996.25) = -29^{\circ}00'28.''118\ , \qquad (1)$$

with an absolute uncertainty of 12 mas (Reid et al. 1999). After removal of the Galactic rotation, the upper limit to any proper motion intrinsic to Sgr A* is about ± 15 km s^{-1}. This implies that our basic understanding of Galactic structure seems to be correct and that Sgr A* is indeed located in the center of the Galaxy.

These observations also provide a lower bound to Sgr A*'s mass. Clearly, most stellar objects in this region have transverse velocities that statistically should peak around 100 - 200 km s^{-1}—an order of magnitude greater than the upper limit for Sgr A*; in the vicinity of this object, stellar motions reach 1,000 km s^{-1}, or more. Assuming no central point mass and an equipartition of the momentum (Reid et al. 1999) between the fastest stars ($m_* v_*$) and Sgr A* ($M_{\rm Sgr\,A^*}\, v_{\rm Sgr\,A^*}$) one naively infers a mass

$$M_{\rm Sgr\,A*} \gtrsim 1,000\, M_\odot \left(\frac{m_*}{10\, M_\odot}\right) \left(\frac{v_*}{1,500\,{\rm km/s}}\right) \left(\frac{v_{\rm Sgr\,A*}}{15\,{\rm km/s}}\right)^{-1}\,, \tag{2}$$

arguing for a non-stellar nature of Sgr A*. This rules out any possible identification with a pulsar or a neutron star.

Simple N-body simulations by Reid et al. (1999) show that the momentum exchange between the stars and Sgr A* during close encounters probably offers the dominant contribution to the latter's proper motion, which for a $2.6\times10^6 M_\odot$ black hole is less than 0.1 km s^{-1}, i.e., consistent with the observations. On the other hand, if Sgr A* did not mark the location of the dark mass, it would certainly feel its potential. To avoid seeing any motion in Sgr A* one would have to conclude either that its orbit around a compact mass is extremely small ($\ll 1$ mas)—thus requiring essentially a point mass again—or that the mass distribution is rising extremely steeply (i.e., a Plummer model with $\alpha = 5$) between the VLBI scale (~ 1 mas, 4×10^{-5} pc) and the stellar motion scale (300 mas, $\sim$0.01 pc). Again, even in this very contrived case the N-body simulations require a strict lower limit of 1,000 $M_\odot$ for Sgr A*.

The NIR stellar proper motion studies and the radio positional measurements of Sgr A* are complementary. Together, they constitute a compelling argument in favor of Sgr A* defining the dynamical center of the central star cluster, and therefore of the Galaxy. In this respect, it might be worth considering shifting the origin of the Galactic coordinate system ($l = 0, b = 0$) to the location of Sgr A*.

3.4 Size Constraints and the Brightness Temperature

The main problem in determining the size of Sgr A* is that its true structure is washed out by scattering in the interstellar medium (Davies, Walsh, & Booth 1976; van Langevelde et al. 1992; Yusef-Zadeh et al. 1994; Lo et al. 1998), leading to a λ^2 dependence of its diameter as a function of the observed wavelength (Fig. 9). Some of the underlying theory is discussed in Romani, Narayan, & Blandford (1986). The scattering is anisotropic, possibly because of large scale magnetic fields pervading the inner Galaxy (Yusef-Zadeh et al. 1994), with a roughly constant ratio between the major and minor axes of 0.53 at all frequencies below 43 GHz and a constant position angle of $80 \pm 3^\circ$. The functional form of the scattering size is given by Lo et al. (1998) as

$$\theta_{\rm minor} = 0.76\,{\rm mas}\ (\lambda/{\rm cm})^2 \quad \theta_{\rm major} = 1.42\,{\rm mas}\ (\lambda/{\rm cm})^2\ , \tag{3}$$

and the scattering size apparently has not changed over a decade (Marcaide et al. 1999).

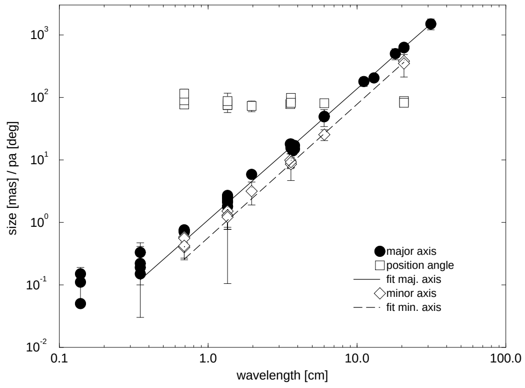

Figure 9 The major source axis (filled circles) of Sgr A*, the minor source axis (open diamonds) and the position angle of the major axis (open squares) as measured by VLBI plotted versus wavelength. (From Krichbaum et al. 1999.)

However, it is possible to constrain the mm-to-sub-mm *intrinsic* size of Sgr A* to within a factor of 10. From the absence of refractive scintillation, Gwinn et al. (1991) have argued that Sgr A* must be larger than 10^{12} cm at $\lambda\lambda 1.3$ and 0.8mm. An upper limit to its size comes from VLBI observations at mm-wavelengths. Because of the low elevation of Sgr A* in most of these observations, the NS resolution is usually much poorer than the EW resolution. The problem of interpreting an elongated source structure in Sgr A* with insufficient baseline coverage is discussed in Doeleman et al. (1999) and Bower et al. (1999b). The most recent measurements were carried out by Bower & Backer (1998), who find a source size of 9×10^{13} cm at 43 GHz (λ7mm)—a mere 2 σ above the scattering size. Significantly, Lo et al. (1998) infer an elongated source in the North-South direction with a size of $5.5 \times (1.5 \times 10^{13}$ cm). Together, these results indicate a 4 σ deviation from the scattering size and, perhaps unexpectedly, appears in the minor axis size dependence. Finally, observations at 86 GHz (λ3mm) and 215 GHz (λ1.4mm) (Rogers et al. 1994; Krichbaum et al. 1998; Doeleman et al. 2001) demonstrate that Sgr A* is compact on a scale at or below 0.1 mas (1.3×10^{13} cm) for the highest frequencies. This corresponds to ~ 17 Schwarzschild radii for a $2.6 \times 10^6\ M_\odot$ black hole. While the exact size of Sgr A* cannot yet be stated with absolute certainty, the latest observations fuel hopes that somewhere in the millimeter wave regime the intrinsic source size will finally dominate over interstellar broadening, allowing a direct comparison with the predictions of various emission theories (see § 5).

The upper limit to Sgr A*'s size (~ 1 A.U.) requires that its brightness temperature be greater than $\sim 10^{10}$ K. Its minimum size of ~ 0.1 A.U. corresponds to an upper limit on the brightness temperature (at 0.8 mm) of about 0.5×10^{12} K. Sgr A* therefore is within the range of typical AGN radio cores (Readhead 1994) and shines below the Compton limit (at approximately 10^{12} K; Kellermann & Pauliny-Toth 1969). This is the maximum brightness temperature of incoherent synchrotron emission from an electron plasma. Above this temperature, the radiation is heavily Comptonized to a frequency well beyond the GHz range. However, if the emitting particles are Maxwellian, they must reach relativistic energies, i.e., their temperature must exceed $\sim 5 \times 10^9$ K, in order for them to be efficient synchrotron emitters (see, e.g., Melia 1992; Melia 1994; Mahadevan, Narayan, & Yi 1996), corresponding to electron Lorentz factors of a few and possibly hundreds.

*3.5 The Spectrum of Sgr A**

After intense radio observation of this source over many years, the spectrum of Sgr A* at these wavelengths is rather well known. Unfortunately, several claims of counterpart identification at shorter wavelengths (NIR, MIR, X-rays) have turned out to be chance associations with other sources (Eckart et al. 1992; Rosa et al. 1992; Goldwurm et al. 1994; Stolovy, Hayward, & Herter 1996).

Duschl & Lesch (1994) compiled an average radio spectrum from the published data and claimed a rough $\nu^{1/3}$ power-law. However, in simultaneous multi-frequency VLA observations (e.g., Wright & Backer 1993; Morris & Serabyn 1996; Falcke et al. 1998), the actual spectrum is seen to be bumpy and the spectral index at GHz frequencies varies between $\alpha = 0.1 - 0.4$ ($S_\nu \propto \nu^\alpha$) (Brown & Lo 1982; Falcke 1999). There may be a low-frequency turnover of the spectrum around 1 GHz (Davies, Walsh, & Booth 1976), the nature of which has never been clarified in detail, though several suggestions (i.e., due to a scattering size that is too large, free-free absorption, and self-absorption) have been proposed. At very low frequencies (e.g., 330 MHz) the entire Sgr A region suffers from free-free absorption (Pedlar et al. 1989).

At high frequencies, Sgr A*'s spectrum must also drop off steeply due to its faintness in the infrared, which is somewhat out of character for an AGN, as first noted by Rieke & Lebofsky (1982). One of the most interesting features currently under study is the suggestion of a sub-millimeter bump in the spectrum (Zylka, Mezger, & Lesch 1992; Zylka et al. 1995; Serabyn et al. 1997) since in all emission models the highest frequencies correspond to the smallest spatial scales, so that the sub-millimeter emission is almost certainly coming directly from the vicinity of the black hole (Melia 1992; Melia 1994).

However, the existence of this bump has been uncertain due to the variability of Sgr A*. In 1996, the spectrum of Sgr A* was measured simultaneously from $\lambda 20$ cm to $\lambda 1$ mm, with four different telescopes (VLA, BIMA, Nobeyama 45 m, & IRAM 30 m), on three continents. The results of this campaign are incorporated into the averaged data plotted in Figure 10, which shows Sgr A*'s spectrum ranging from 1.36 to 232 GHz.

The spectrum at lower frequencies was adequately described by two power-laws with spectral indices $\alpha = 0.17$ ($S_\nu \propto \nu^\alpha$) between 1.36 GHz and 8.5 GHz and $\alpha = 0.30$ between 15 and 43 GHz. The 20 year average spectral index of Sgr A* in the range $1.4 - 22$ GHz is $\alpha = 0.28$, as derived by Zhao, Bower, & Goss (2001). The spectral index of Sgr A* increases to $\alpha = 0.52$ in the mm-range, while the $\lambda 3$-to-2 mm spectral index becomes even higher, reaching $\alpha = 0.76$. Based on these results, one can safely conclude that there probably exists a significant mm-excess in the spectrum of Sgr A*, or possibly even a separate component at these frequencies. So far no bright confusing source has been found in high-resolution millimeter-wave maps that could explain such an excess as being extrinsic to Sgr A* (e.g., Zhao & Goss 1998). However, it is possible that the excess, seen also as a curvature in time-averaged spectra, is in part due to large-amplitude flares at high frequencies (Tsuboi, Miyazaki, & Tsutsumi 1999).

In the sub-mm range, detections exist up to 666 GHz (Zylka et al. 1995)

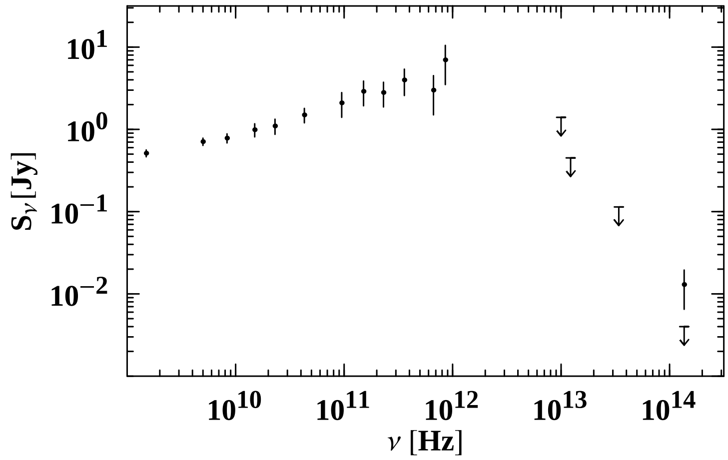

Figure 10 Time-averaged spectrum—flux density versus frequency—of Sgr A* from radio to the near infrared. The radio data up to 22 GHz are from Zhao et al. (2001) averaged over 1980-2000; 43 & 95 GHz data are the averages from the campaign of Falcke et al. (1998); 230 & 350 GHz data are from Zylka et al. (1995) averaged over 1987-1994, and 1991-1994, respectively; the remaining data are discussed in the text. The error bars indicate variability (one standard deviation), assumed to be at least 50% beyond 350 GHz.

with a flux density of up to $3 - 4$ Jy. Serabyn et al. (1997) claim a 7 ± 2 Jy detection at 850 GHz while only upper limits exist in the mid-infrared: < 1.4 Jy at 30 μm (Telesco, Davidson, & Werner 1996), $< 450 \pm 150$ mJy at 24.5μm and $< 114 \pm 30$ mJy at 8.81 μm (Cotera et al. 1999)[1]. In the near-infrared, Genzel & Eckart (1999) give an upper limit of 4 mJy at 2.2 μm, with an (as yet unconfirmed) detection around 13 mJy of Sgr A* in certain epochs (all flux densities are dereddened). In the optical, of course, Sgr A* is reddened by an $A_V = 30$ and hence undetectable. A time-averaged spectrum from 1.4 GHz to 10^{14} Hz is shown in Figure 10.

In the X-rays, *ROSAT* detected emission at the position of Sgr A* (Predehl & Trümper 1994), but with a rather large beam that might have included some diffuse emission as well. The luminosity in the 0.2-2 keV range was about $1 - 2 \times 10^{34}$ erg s^{-1} for standard Galactic reddening (Predehl & Zinnecker 1996). Recently *Chandra* detected a source within $1''$ of Sgr A* with a rather low X-ray luminosity of about 0.9×10^{34} erg s^{-1} in the 0.5-10 keV band for a photon index of $2.75^{+1.25}_{-1.0}$ (Baganoff et al. 2001). This appears to be the first convincing detection of Sgr A* in an energy range different from radio. There is also γ-ray emission at a level of $(2.2 \pm 0.2) \times 10^{37}$ erg s^{-1} above 100 MeV (Mayer-Hasselwander et al. 1998) from the Sgr A region. This level should be considered an upper limit for Sgr A* because of the possibly very large extent ($\sim 1.5^\circ$) of the emitter and the lack of detected variability. Finally, there is also a claimed excess of high-energy neutrons ($\sim 10^{18}$ eV) seen in air showers toward the direction of the Galactic Center (Hayashida et al. 1999), which may, however, also come from a relatively large region.

[1] These flux densities were dereddened by a factor $10^{(A_\lambda/A_V)\times A_V \times 0.4} \sim 5.7$ for an $A_V = 30$, using the extinction law given in Rieke & Lebofsky (1985) and Mathis (1990), with $A_{8.81\mu m}/A_V = 0.063$ and $A_{24.5\mu m}/A_V = 0.014$

*3.6 Radio Variability of Sgr A**

An important parameter for constraining the spectrum and nature of Sgr A* is its variability. In the radio flux density, variations are clearly seen between different epochs, but the time scale of the variability at various frequencies is not well determined and it is not clear whether some of the more extreme claims of variability are real or instrumental artifacts. Zhao et al. (1989) and Zhao et al. (1992) found a number of outbursts at higher frequencies and a rather low level of variability at low frequencies.

Falcke (1999) published the results of 540 daily observations of Sgr A* at 2.3 and 8.3 GHz with the Green Bank Interferometer (GBI). A peak-to-peak variability of 250 mJy with an RMS (i.e., modulation index) of 6% and 2.5% at 8.3 and 2.3 GHz respectively was found. The median spectral index between the two observed frequencies (8.3 and 2.3 GHz) for the whole period was $\alpha = 0.28$ ($S_\nu \propto \nu^\alpha$), varying between 0.2 and 0.4. There is a clear trend for the spectral index to become larger when the flux density in both bands increases. The spectral index versus flux correlation and the different modulation indices at the two frequencies imply that outbursts in Sgr A* are more pronounced at higher frequencies. This is not consistent with a simple model of refractive interstellar scintillation as suggested by Zhao et al. (1992): the variability time scale inferred at 2.3 GHz and 8.3 GHz is comparable to that found at 5 GHz by Zhao et al. (1992) and it does not follow a $t \propto \lambda^2$ law.

The most direct conclusion one can draw from the variability data is the high degree of correlation between emission at 2.3 and 8.3 GHz. The lag is apparently less than three days which corresponds to a light travel distance of $\leq 10^{16}$ cm (~ 60 mas at the distance to the Galactic Center; this is less than the scattering size). For models that have a frequency-dependent structure (e.g., the accretion and jet models) this will be an upper limit to the size of the emitting region at these frequencies. At both frequencies the characteristic time scale is somewhere between 50 and 250 days. There is very little variability on time scales of a few days below 10 GHz and a slow, linear increase of the flux density is observed over the entire 2 years of observations.

Recently Zhao, Bower, & Goss (2001) have investigated 20 years of VLA data and find marked outbursts with an amplitude around 0.4 Jy at 23 GHz with a characteristic time scale of less than 25 days that are not seen below 8 GHz. The flare amplitude seems to increase with frequency. Similar flares at mm-waves have also been observed by Tsuboi, Miyazaki, & Tsutsumi (1999) and Wright & Backer (1993) even though mm-wave flux densities are notoriously difficult to calibrate. An intriguing result that needs further confirmation is the possibility that these high-frequency flares are periodic (or perhaps quasi-periodic) with a period around 106 days (Zhao, Bower, & Goss 2001). A theoretical interpretation for these variability characteristics is provided in § 4 below.

*3.7 The Measured Linear Polarization of Sgr A**

Early papers that discussed the radio emission of Sgr A did not report any significant polarization. Ekers et al. (1975) quoted an upper limit of 1% linear polarization for the region of peak emission in Sgr A, which at that time was not well resolved in their 5 GHz Westerbork observations. Subsequent observations with the VLA similarly yielded a null polarization measurement (Yusef-Zadeh &

Morris 1987). This was in contrast to the situation with AGNs, in which the linear polarization is typically a few percent (Hughes, Aller, & Aller 1985; Marscher & Gear 1985). So, while the measurement of polarization promises useful information, the early negative results for Sgr A* made this a non-issue for over a decade.

One reason why the linear polarization in Sgr A* is low could be the presence of a scattering screen between the Galactic Center and the observer, which depolarizes the radiation. This can come about because (1) the differential Faraday rotation of the homogeneous medium may be so high that within the bandwidth of the observation the polarization vector is rotated by more than 180 degrees and therefore is largely canceling itself (see below), and (2) there may be considerable variation of the Faraday rotation in the scattering screen so that every ray that reaches the observer gets rotated differently, which reduces the overall polarization significantly. In this context, it may be relevant to ask whether such an effect could lead to a conversion from linear to circular polarization; after all, we have an anisotropic scattering screen permeated by a large scale magnetic field (Yusef-Zadeh et al. 1994).

Bower et al. (1999a) have reported the results of continuum polarimetry at 4.8 GHz and spectro-polarimetry at 4.8 and 8.4 GHz, using the VLA. The spectro-polarimetric observations were made to exclude strong differential Faraday rotation in the Galactic Center that could lead to a de-polarization of the radiation when observed in continuum mode integrating over a large bandwidth. Faraday rotation is produced when radio waves pass through an ionized and magnetized medium. Since left and right circularly polarized waves have different refractive indices for a given magnetic field orientation, a wavelength-dependent delay is induced which rotates the position angle $\phi_{\rm LP}$ of the linear polarization vector, yielding $\phi_{\rm LP} = {\rm RM}\lambda^2$. The parameter RM is called the rotation measure and can be determined by measuring the position angle of the linear polarization vector $\phi_{\rm LP}$ at different wavelengths λ. For a given frequency bandwidth $\Delta\nu$, significant de-polarization is obtained if $\phi_{\rm LP}$ changes by more than one radian, i.e., if ${\rm RM} > 0.5\nu/(\lambda^2\Delta\nu)$. This means that for a typical VLA bandwidth of 50 MHz at 4.8 GHz, the critical rotation measure is $\sim 10^4$ rad m^{-2}, which is not deemed to be so excessively high that it could not be present in the Galactic Center.

The results of the broad-band continuum polarimetry indeed confirmed the absence of linear polarization with a rather low upper limit of $< 0.1\%$ fractional polarization. By Fourier transforming the spectro-polarimetric data to sample multiple rotations of the polarization vector across the entire band, Bower et al. (1999a) were able to exclude Faraday rotation as the cause of this, with RM values up to 10^7 rad m^{-2}. To further clarify whether RM fluctuations in the scattering medium could de-polarize the radiation from Sgr A*, one could simply try to measure the linear polarization at progressively higher frequencies. Since the scattering size decreases with ν^{-2} the differential changes in the angles to the line of sight for light rays from Sgr A* will rapidly become smaller and smaller with increasing wavelength. In addition the Faraday rotation itself will also decrease with ν^{-2}. Bower et al. (1999c) and Bower et al. (2000b) have sought high-frequency polarization of Sgr A* with the VLA and found only upper limits. So de-polarization of the radiation from Sgr A* by the scattering medium appears to be rather unlikely at present.

The situation at sub-mm wavelengths could be different. The most recent information is provided by linear polarization measurements using the SCUBA

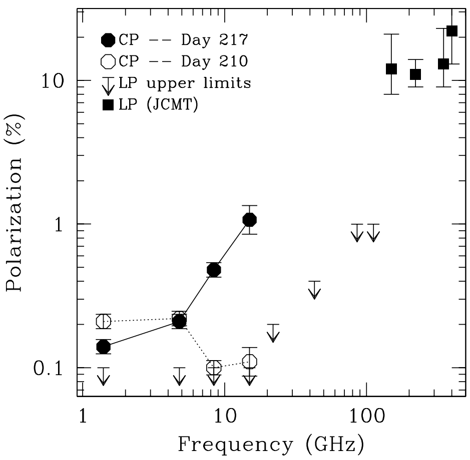

Figure 11 Linear and circular polarization in Sgr A* from 1.4 to 86 GHz. The down arrows indicate upper limits for linear polarization measurements. The open octagons are CP measurements from the VLA on July 28, 1999. The filled octagons are measurements from the VLA on August 5, 1999. The sign of CP has been flipped in this figure. Also shown is the 10+9-4% detection of LP at 150 GHz by Aitken et al. (2000). (From Bower 2000.)

camera at the James Clerk Maxwell Telescope (JCMT), at 0.75, 0.85, 1.35, and 2 mm (Aitken et al. 2000). These authors have reported the detection of fractional linear polarization as high as 10% at these wavelengths. However, one potential problem with these low-resolution observations is the possible confusion of the Sgr A* flux with that from dust emission in the surrounding circumnuclear disk and from the mini-spiral in Sgr A West. If confirmed, the lack of a detected polarization at λ3.5 mm and λ2.7 mm, in contrast to these detections at shorter wavelengths, may be a possible signature of compact sub-mm emission from within several Schwarzschild radii of the black hole (Aitken et al. 2000; Quataert & Gruzinov 2000a; Agol 2000; Melia, Liu, & Coker 2000).

*3.8 The Measured Circular Polarization of Sgr A**

In synchrotron sources, the degree of circular polarization is $m_c < 0.1\%$; only rarely has m_c reportedly reached 0.5% (Weiler & de Pater 1983). The degree of circular polarization usually peaks near 1.4 GHz and decreases strongly with increasing frequency.

Given the stringent upper limits on the linear polarization of Sgr A* at cm-wavelengths, the detection of circular polarization came as somewhat of a surprise (Bower, Falcke, & Backer 1999). The circular polarization in Sgr A* was found to be $m_c = -0.36 \pm 0.05\%$ and $m_c = -0.26 \pm 0.06\%$ at 4.8 and 8.4 GHz. The detection was quickly confirmed by Sault & Macquart (1999), using the Australia Telescope Compact Array at 4.8 GHz.

The circular polarization is variable on a ten day time scale and is now detected up to 43 GHz (Bower et al. 2000a; Bower 2000). The overall spectrum of circular polarization seems to be inverted and increases beyond 8 GHz (see Fig. 11).

Polarimetric measurements of Sgr A* are opening up a relatively new and exciting field. The first attempts at interpreting the polarization properties of this source are just being made (Agol 2000; Quataert & Gruzinov 2000a; Melia, Liu, & Coker 2000; Beckert & Falcke 2001) and some of these are discussed below in § 5.

4 GAS DYNAMICS AND STELLAR WIND CAPTURE

Having described the key observational characteristics of Sgr A*, let us now turn our attention to the physical interpretation of this object. As we alluded to in the previous section, the abundance of gas in the environment surrounding Sgr A* clearly points to accretion as the incipient cause of its ensuing energetic behavior. The properties described above are consistent with the idea that Sgr A*'s spectrum results from the energy liberated by a compressed hot plasma either bound to the central gravitational potential during infall (see § 5.1), or in the process of expulsion in the form of a jet (see § 5.2). However, we shall first play the "devil's advocate" and consider the possibility that the potential well is instead associated with a distributed cluster of dark objects (rather than a single point mass; Melia & Coker 1999), and then compare the results with the expectations for a black hole potential.

The Galactic Center wind appears to be produced by the early-type stars enclosed (in projection) within the Western Arc, the Northern Arm, and the Bar. Thus far, 25 such stars have been identified (Genzel et al. 1996), and all appear to be located within the central parsec surrounding Sgr A*. Figure 12 shows the positions (relative to Sgr A*) of these wind sources, in which the size of the circle marking each position corresponds to the relative mass loss rate (on a linear scale) for that star. Note that due to clustering some of the stars are combined into a single wind source in this figure, and some are outside the field of view.

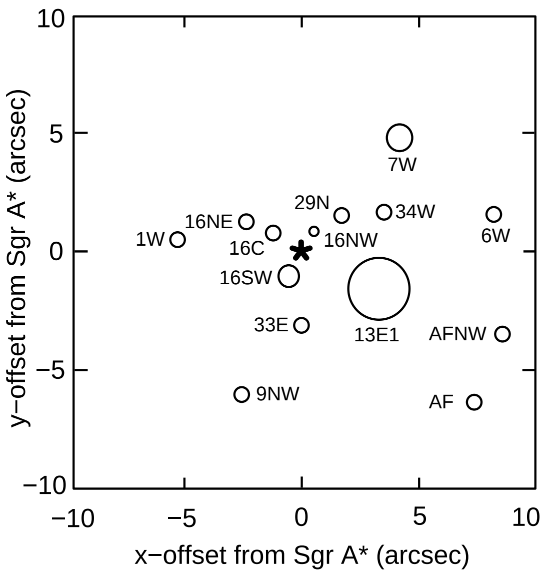

Figure 12 Location of some of the wind-producing stars relative to the position of Sgr A* indicated by the * symbol. The radius of each circle corresponds (on a linear scale) to that star's mass loss rate. Setting the scale is 13E1, with $\dot{M} = 7.9 \times 10^{-4}\ M_\odot\ \mathrm{yr}^{-1}$. (From Coker & Melia 1997.)

The gravitational potential of a dark cluster can be represented by an "η-model" (Haller & Melia 1996). This function mimics an isotropic mass distribution with a single parameter, and it is scaled so that the total dark cluster mass within 0.01 pc is $2.6 \times 10^6\ M_\odot$. Melia & Coker (1999) used the 3D hydrodynamics code ZEUS to simulate the flow of the Galactic Center wind through this distributed dark matter using the η-potential, and one of the key results of this calculation is summarized in Figure 13, which shows the angle- and volume-averaged density and temperature for the whole central $0.''7$ region, using a bin size of $0.''0025$. In this figure, the density rises gradually to the middle, and reaches an average value of roughly 10^8 cm^{-3}. In contrast, the central density for a gas falling freely into a black hole potential with the same central mass approaches $\sim 10^{13}$ cm^{-3} (Melia 1994). The temperature similarly rises to the middle, but it levels off within about 0.004 pc, and the average is never greater than about 10^7 K. This is to be compared with the temperature profile of the gas falling into the black hole, where T attains values as high as 10^{10} K or more. This is critical because the electrons begin to emit significantly via the synchrotron process when they become relativistic above a few times 10^9 K. This gas can at best therefore only emit cyclotron radiation, but the emissivity is a strong function of T and is here insignificant compared to bremsstrahlung. The flattening of the density and temperature profiles shown in Figure 13 is a direct consequence of the shallowness of the cluster potential compared to the steep potential gradients encountered by the gas falling into the black hole. The magnetic field, which is coupled to the physical state of the gas, behaves in a similar fashion, though it is clumpier due to the uneven dissipation in regions of gas compression and rarefaction.

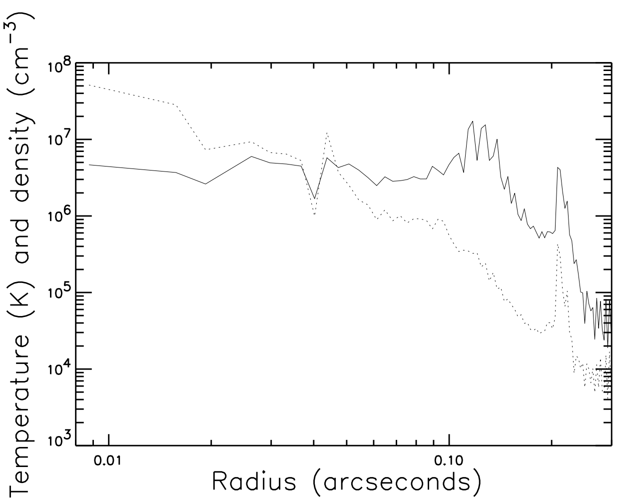

Figure 13 Angle- and volume-averaged density (dotted) and temperature (solid) as a function of radius (in arcseconds) from the center. The flattening of these distributions at small radii (i.e., $< 0.''1 \approx 0.004$ pc) is clearly evident. (From Melia & Coker 1999.)

Gas flowing through a dark cluster may get trapped, but it clearly does not produce the type of condensation and high temperature required to account for Sgr A*'s spectrum. This is indirect support for the inference drawn from other lines of evidence that the dark matter is instead concentrated in the form of a single compact object.

Let us therefore consider the physical state of the gas when the gravitational potential well deepens as the plasma approaches the event horizon. In the classical Bondi-Hoyle (BH) scenario (Bondi & Hoyle 1944), the mass accretion rate for a uniform hypersonic flow is $\dot{M}_{BH} = \pi {R_A}^2 m_H n_w v_w$, in terms of the accretion radius $R_A \equiv 2GM/{v_w}^2$. With the conditions at the Galactic Center (see above), we would therefore expect an accretion rate $\dot{M}_{BH} \sim 10^{21}$ g s^{-1} ($\approx 1.6 \times 10^{-5}\ M_\odot$/yr) onto the black hole, with a capture radius $R_A \sim .02$ pc.

In reality the flow past Sgr A* is not likely to be uniform, since one might expect many shocks to form as a result of wind-wind collisions within the IRS 16 complex, even before the plasma reaches R_A. The implications for the spectral characteristics of Sgr A*, and thus its nature, are significant. Coker & Melia (1997) have therefore undertaken the task of simulating the BH accretion from the spherical winds of a distribution of 10 individual point sources located at an average distance of a few R_A from the central object. The results of these simulations show that the accretion rate depends not only on the distance of the mass-losing star cluster from the accretor but also on the relative spatial distribution of the sources. In addition, the co-existence of hot and warm gas components may itself alter the Bondi-Hoyle capture profile (Baganoff et al. 2001), which is not included in these simulations. The capture rate inferred by these authors is $\approx 3 \times 10^{-6}\ M_\odot$/yr.

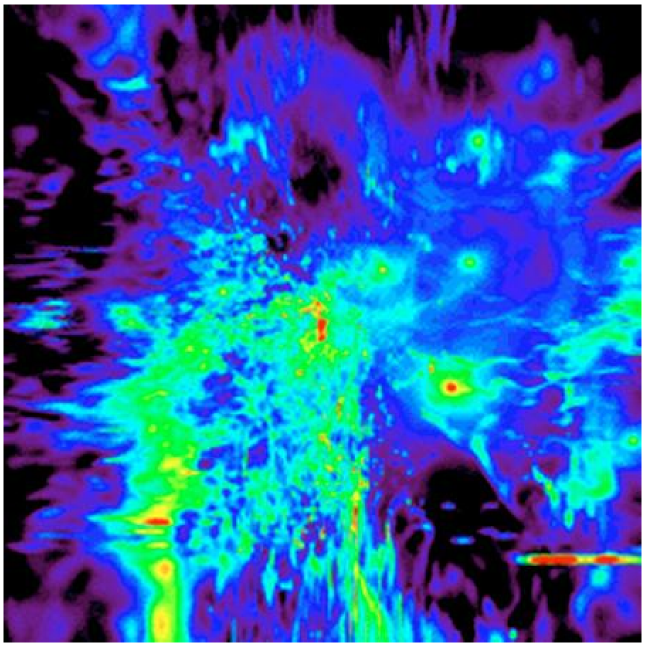

Figure 14 A "snapshot" of the column density (i.e., the gas density integrated along the line of sight) taken at a point in the calculation when the gas distribution had reached stationary equilibrium. Sgr A* is in the middle, and the dimensions are approximately 0.5 light years on each side. Some 15 to 20 stars surrounding the black hole each produce an efflux of gas (i.e., "winds"), which collide and form this tessellated pattern of gas condensations, some of which are captured by the black hole and accrete towards it. Several of the wind-producing stars are visible to the right of the image. The color scale is logarithmic, with red corresponding to a column density of 10^{21} g cm^{-2}, then yellow, blue, and black, which corresponds to 10^{16} g cm^{-2}. (From Coker & Melia 1997.)

Figure 14 shows a logarithmic color scale image of the density profile for a slice running through the center of the accretor, for one of these simulations taken 2,000 years after the winds are "turned on". Once the stellar winds have cleared the region of the original low density gas, all such simulations point to an overall average density ($\sim 10^3$ cm^{-3}) in agreement with observations.

Figure 15 shows the mass accretion rate, $\dot{M}$, and the accreted specific angular momentum, λ (in units of cr_s, where r_s is the Schwarzschild radius), versus time, starting 2 crossing times ($\sim$ 800 years) after the winds are "turned on". The average value for the mass accretion rate once the system has reached equilibrium is $\dot{M} = 2.1 \pm 0.3 \dot{M}_{BH}$.

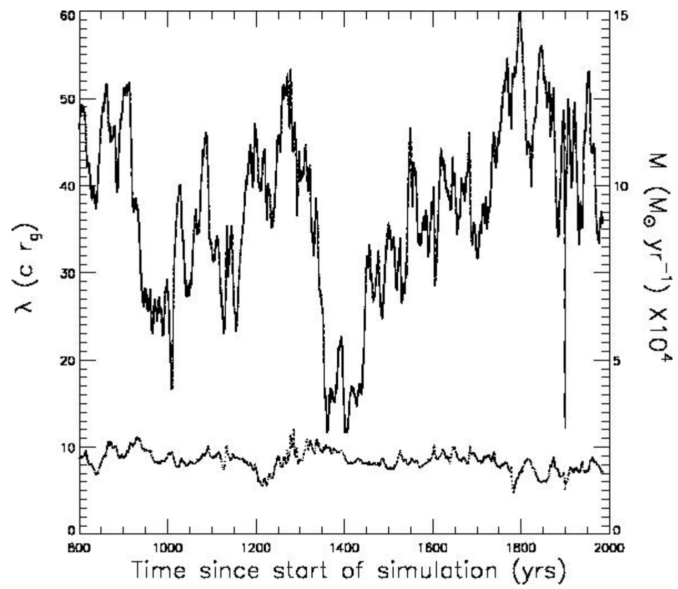

Figure 15 The upper solid curve is the *magnitude* of the accreted specific angular momentum λ (in units of cr_s). The scale for λ is on the left side. The lower dotted curve is the mass accretion rate $\dot{M}$ (10^{-4} $M_\odot$ yr^{-1}) versus time. The scale for $\dot{M}$ is shown on the right side. (From Melia & Coker 1999.)

The mass accretion rate shows high frequency temporal fluctuations (with a period of $\lesssim 0.25$ yr) due to the finite numerical resolution of the simulations. The low frequency aperiodic variations (on the order of 20% in amplitude) reflect the time dependent nature of the flow. Thus, the mass accretion rate onto the central object, and consequently the emission arising from within the accretor boundary, is expected to vary by $\lesssim 20 - 40\%$ (since in some models the luminosity may vary by as much as $\propto \dot{M}^2$) over the corresponding time scale of < 100 years, even though the mass flux from the stellar sources remains constant. The temporal variations in Sgr A*'s radio luminosity (§ 3.6) are probably due (at least in part) to these fluctuations in the accretion rate toward small radii.

Similarly, the accreted λ can vary by 50% over $\lesssim$ 200 years with an average equilibrium value of 37 ± 10. It appears that even with a large amount of angular momentum present in the wind, relatively little specific angular momentum is accreted. This is understandable since clumps of gas with a high specific angular momentum do not penetrate to within 1 R_A. The variability in the sign of the components of λ suggests that if an accretion disk forms at all, it dissolves, and reforms (perhaps) with a different sense of spin on a time scale of ~ 100 years or less.

The captured gas is highly ionized and magnetized, so it radiates via bremsstrahlung, cyclo-synchrotron and inverse Compton processes. However, the efficiency of converting gravitational energy into radiation is quite small (as little as 10^{-4} in some cases), so most of the dissipated energy is carried inwards (Shapiro 1973; Ipser & Price 1982; Melia 1992; Melia 1994). In fact, if the magnetic field is a negligible fraction of its equipartition value (see below), Sgr A* would be undetectable at any frequency, except perhaps at soft X-ray energies. But as the plasma continues to compress and fall toward smaller radii, one or more additional things can happen, each of which corresponds to a different theoretical assumption, and therefore a potentially different interpretation, which we explore in the next section.

5 EMISSION MODELS FOR SGR A*

5.1 Emission due to the Accreting Plasma

The questions one may ask include the following: (1) Does the flow carry a large specific angular momentum (in contrast to our expectations from the Bondi-Hoyle simulations) so that it forms a disk with lots of additional dissipation? (2) Does the flow produce a radiatively dominant non-thermal particle distribution at small radii (e.g., from shock acceleration), or does thermal emission continue to dominate the spectrum? (3) Does the flow lead to an expulsion of plasma at small radii that forms a non-thermal jet, which itself may then dominate the spectrum? These, either individually or in combination, have led to a variance of assumptions about the nature of the inflowing gas that then form the basis for the development of different interpretations.

Observationally, one of the key issues is why the infalling gas maintains a low radiative efficiency. In the picture developed by Narayan, Yi, & Mahadevan (1995), and updated in Narayan et al. (1998), the infalling gas is assumed to carry a very large angular momentum towards the center, forming a big accretion disk (with an outer edge extending beyond 10^5 Schwarzschild radii or so). The Bondi-Hoyle simulations discussed above suggest that clumps of gas with relatively large specific angular momentum do not penetrate inwards. However, a large disk may form if the viscosity is anomolously high even at large radii. In this case, the overall emission must now include the additional dissipation of the captured angular momentum. To comply with the observed low efficiency of Sgr A*, this model therefore also assumes that the electron temperature is much lower than that of the protons ($T_e \ll T_p$). In fact, $T_e < 10^{10}$ K. Since the electrons do the radiating, the efficiency remains small even though the protons are very hot. It is important to point out, in this regard, that the success or otherwise of an advection-dominated model rests on whether or not event horizons really do exist. The low efficiency of such an inflow can be maintained only if the energy transported inward vanishes from view Narayan et al. (1998).

Large accretion disks such as this are known as ADAFs. Strictly speaking, the acronym ADAF stands for Advection Dominated Accretion Flow, which embraces all forms of accretion (disk or otherwise) in which a large fraction of the dissipated energy is advected inwards by the hot protons, rather than radiated away locally by the electrons. So for example, if the gas flow is quasi-spherical until it gets to within a handful of Schwarzschild radii (as suggested by the Bondi-Hoyle simulations) it may still be advection-dominated if the emissivity of the gas is very low; this may occur when the magnetic field is weak (Kowalenko & Melia 1999; Coker & Melia 2000; see below). In practice, however, the term ADAF is conventionally used to denote the category of accretion patterns that involve a large, two-temperature *disk*.

Not surprisingly, the radiative and dynamic properties of ADAFs are sensitive to the outer boundary conditions, which are not well known. In their analysis, Yuan et al. (2000) adopted T_e, T_p, and the specific angular momentum of the accretion flow at the outer boundary as their principal free parameters. Allowing these variables to range over reasonable values produces differences of several orders of magnitude in the peak radio, IR, and X-ray fluxes. An additional complication is the possible "contamination" of the thermal particle distribution with non-thermal particles produced, e.g., from the decay of charged mesons, which are themselves created through proton-proton collisions (Markoff, Melia, & Sarcevic 1997; Markoff, Melia, & Sarcevic 1999; Mahadevan 1999). Nonetheless, ADAF models can be designed to give reasonable fits to the data (Menou, Quataert, & Narayan 1999), though the recent Chandra X-ray measurements seem problematic (see below).

An important evolution in the ADAF theory came with the realization that when a black hole accretes gas conservatively at a rate well below the Eddington value (so that its radiative efficiency is very low), the net enery flux, including the energy transported by the viscous torque, is likely to be close to zero at all radii (Blandford & Begelman 1999; see also Narayan & Yi 1994). In other words, a large fraction of the plasma in an ADIOS (i.e., an Advection Dominated Inflow/Outflow Solution) may be unbound, leading to significant mass loss in the form of a wind. As such, the assumption of a constant accretion rate throughout the ADAF region may be quite poor. This situation is not unrelated to the Bondi-Hoyle result (Coker & Melia 1997; see previous section) that clumps of gas with large specific angular momentum generally do not accrete inwards. Much of the recent effort in this area has therefore been channelled into producing more detailed, numerical simulations to gauge whether the ADAF idea still remains viable as an explanation for Sgr A*'s radiative characteristics. Several independent groups (Hujeirat 1999; Manmoto et al. 2000; Turolla & Dullemond 2000) who are now investigating the structure of ADAF disks are reporting positive Bernoulli values for a wide range of conditions, indicating that outflows are a necessity, though perhaps not as large as the early ADIOS estimates seemed to suggest; for example, Turolla & Dullemond (2000) report a ratio of inflowing to outflowing mass of about 1/2. Earlier, Igumenshchev, Chen, & Abramowicz (1996) had shown that serious outflows occur only if the viscosity parameter α is 0.3 or larger, which may be unrealistic, leaving somewhat uncertain the issue of whether real outflows occur or not.

As more and more physical details are added to this study, the degree of complexity in the flow grows in corresponding fashion. It now appears that ADAF disks are also convectively unstable for low values of viscosity (Igumenshchev, Abramowicz, & Narayan 2000). Hydrodynamic simulations of such flows reveal a radial density profile that is significantly flatter than that expected for a canonical ADAF. Other recent modifications to the canonical ADAF model include the introduction of ADAFs without turbulent viscosity driving the accretion process. In one such picture (Kino, Kaburaki, & Yamazaki 2000), accretion through the

ADAF disk is instead controlled by a large-scale magnetic field. Another new ingredient is the influence of convection ("CDAF", standing for convective ADAF model), which requires an extremely low accretion rate, around 10^{-8} $M_\odot$ yr^{-1} (Quataert & Gruzinov 2000b; Quataert & Gruzinov 2000a; Narayan, Igumenshchev, & Abramowicz 2000).

A difficulty faced by the ADAF disk model is that there does not appear to be a simple way out of the large dissipation (and consequent radiative efficiency) produced by the wind falling onto the plane (Falcke & Melia 1997). In addition, the ADAF model is yet to be established observationally. ADAF disk models have now been applied extensively to several low-luminosity systems, including the cores of elliptical galaxies, but compelling observational evidence for their existence is lacking. Di Matteo et al. (1999) examined the high-frequency radio observations of NGC 4649, NGC 4472, and NGC4636 and concluded that the new radio limits disagree with the canonical ADAF predictions, which tend to significantly overestimate the observed flux. They concluded that if accretion in these objects occurs in an advection-dominated disk mode, the radio limits imply a strong suppression of the emission from the central regions. This problem may be worse still since the measurements reported in this paper apparently included substantial extended emission (e.g., from the jet) due to the poor spatial resolution of the observations.

A possible resolution to this problem is that the magnetic field within the inflowing gas may be sub-equipartition, which clearly has the effect of lowering the synchrotron emissivity. This effect may be present whether or not the dissipated energy in the flow is advected inwards through the event horizon. The idea that Sgr A*'s low emissivity is due to a sub-equipartition magnetic field B deserves close attention, especially in view of the fact that the actual value of B depends strongly on the mechanism of field line annihilation, which is poorly understood. Two processes that have been proposed are (i) the Petschek mechanism (Petschek 1998), in which dissipation of the sheared magnetic field occurs in the form of shock waves surrounding special neutral points in the current sheets and thus, nearly all the dissipated magnetic energy is converted into the magnetic energy carried by the emergent shocks; and (ii) the tearing mode instability (van Hoven, Hendrix, & Schnack 1995), which relies on resistive diffusion of the magnetic field and is very sensitive to the physical state of the gas. In either case, the magnetic field dissipation rate is a strong function of the gas temperature and density, so that assuming a fixed ratio of the magnetic field to its equipartition value may not be appropriate.

Kowalenko & Melia (1999) have used the van Hoven prescription to calculate the magnetic field annihilation rate in a cube of ionized gas being compressed at a rate commensurate with that expected for free-fall velocity onto the nucleus at the Galactic Center. An example of these simulations is shown in Figure 16, for parameter values like those pertaining to the Galactic Center. Whereas the rate of increase $\partial B/\partial t|_f$ in B due to flux conservation depends only on the rate $\dot{r}$ of the gas, the dissipation rate $\partial B/\partial t|_d$ (based on the van Hoven prescription) is a function of the state variables and is therefore not necessarily correlated with $\dot{r}$. Although these attempts at developing a physical model for magnetic field dissipation in converging flows are still rather simplistic, it is apparent from the test simulations that the equipartition assumption is not always a good approximation to the actual state of a magnetohydrodynamic flow, and very importantly, that the violation of equipartition can vary in degree from large to small radii, in either direction. Coker & Melia (1999) have calculated the cm to mm spectrum produced by a quasi-spherical infall in Sgr A* using its most recently determined mass, and an empirical fit to the magnetic field based on these simulations of magnetic dissipation. Without the additional suppression for the radiative efficiency provided by, e.g., a two-temperature flow, the implied magnetic field intensity in Sgr A* is limited to a value of about $5 - 10$ Gauss.

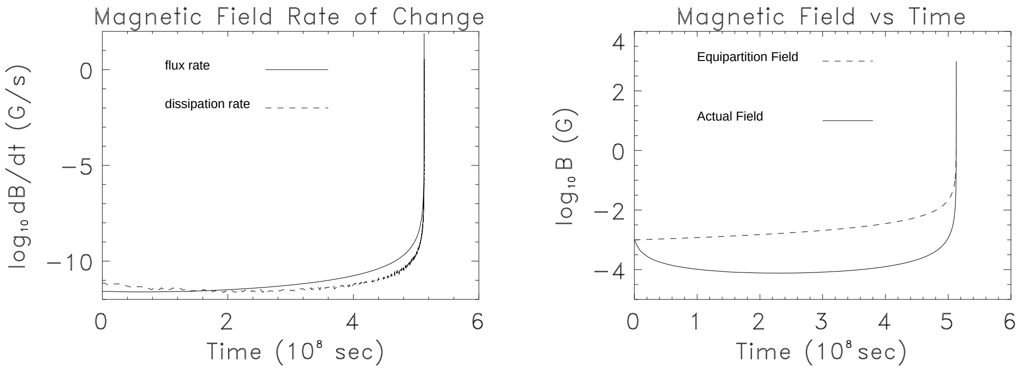

Figure 16 The *left* panel shows the magnetic field rates of change $\partial B/\partial t|_f$ and $\partial B/\partial t|_d$ due, respectively, to flux conservation and resistive dissipation as functions of time in units of 10^8 seconds. The compression rate is here assumed to be the free-fall velocity at the accretion radius. Solid curve: the rate of increase due to flux conservation; dashed curve: the rate of decrease due to resistive dissipation. The *right* panel shows the magnetic field (solid curve) calculated as a function of time from the rates displayed in left panel. By comparison, the equipartition field B_{eq} is shown here as a dashed curve. The rapid increase in B toward the end of the simulation is associated with the accelerated rate of change in the physical parameters as the gas flows inwards toward a zero radius. (From Kowalenko & Melia 1999.)

If Sgr A*'s spectrum is indeed produced by the infalling plasma (as opposed to an outflowing jet, which we consider in the subsequent section), the geometry of the emitting region ought to be tightly constrained by the new polarization measurements described in § 3.7 above. Although the upper limits to the linear polarization in Sgr A* are found to be quite low (less than 1%) below 86 GHz (Bower et al. 1999), this is not the case at 750, 850, 1,350, and 2,000 μm, where a surprisingly large intrinsic polarization of over 10% has now been reported (Aitken, et al. 2000). These observations also point to the tantalizing result that the position angle changes considerably (by about 80°) between the mm and the sub-mm portions of the spectrum, which one would think must surely have something to do with the fact that the emitting gas becomes transparent at sub-mm wavelengths (Melia 1992, 1994).

Agol (2000) constructed a simple two-component model for the radio-to-millimeter spectrum and the polarization in this source. His analysis predicts that the polarization should rise to nearly 100% at shorter wavelengths. The first component, possibly a black hole-powered jet, is compact, of low density, and is self-absorbed near 1 mm, with an ordered magnetic field, a relativistic Alfvén speed, and a non-thermal electron distribution. In his model, the second component is poorly constrained, but may be a convection-dominated accretion flow with 10^{-9} $M_\odot$ yr^{-1}, in which feedback from accretion onto the black hole suppresses the accretion rate at larger radii. This is consistent with the result of Quataert & Gruzinov (2000a), who show that a high-accretion rate ADAF would completely depolarize

Sgr A*.

Melia, Liu, & Coker (2000) have suggested that the mm to sub-mm "excess" in the spectrum of Sgr A* (see Fig. 10) may be the first indirect evidence for the anticipated circularization of the gas falling into the black hole at $5 - 25\ r_s$. In their simulation of the Bondi-Hoyle accretion onto Sgr A* from the surrounding winds, Coker & Melia (1997) concluded that the accreted specific angular momentum $l \equiv \lambda r_s c$ can vary by 50% over $\lesssim$ 200 years with an average equilibrium value in λ of about 30 or less. The fact that $\lambda \neq 0$ therefore raises the expectation that the plasma must circularize toward smaller radii before flowing through the event horizon. Melia, Liu & Coker (2000, 2001) showed that this dichotomy, comprising a quasi-spherical flow at radii beyond 50 r_s or so, and a Keplerian structure toward smaller radii, may be the explanation for Sgr A*'s spectrum, including the appearance of the "excess", which is viewed as arising primarily within the circularized component.

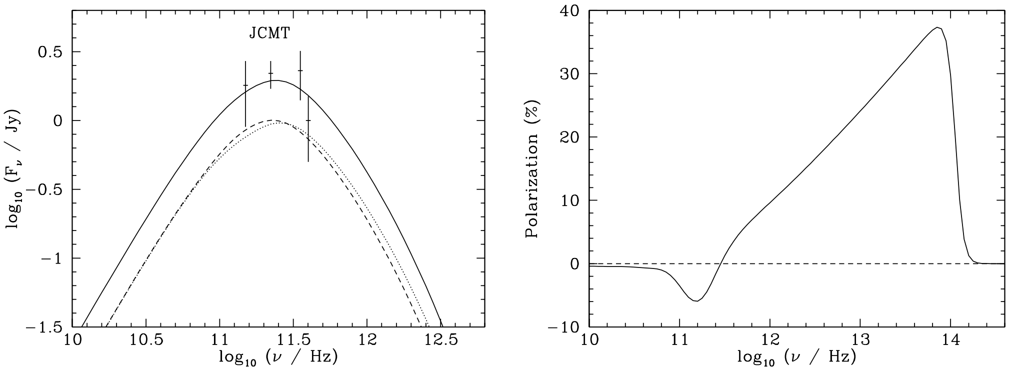

Figure 17 The *left* panel shows the spectrum corresponding to the best fit model. The dotted curve corresponds to the first component and the dashed curve corresponds to the second component. The solid curve is the sum of these two. The *right* panel shows the percentage polarization for this best fit model. (From Melia, Liu & Coker 2000.)

In the best-fit model for the polarized mm and sub-mm emission from Sgr A*, the peak frequency of the flux density is 2.4×10^{11} Hz, and the flip frequency (at which the position angle changes by 90°) is 2.8×10^{11} Hz. Above the peak, the medium is optically thin; it is optically thick at frequencies below it. To understand how the polarization characteristics arise in this context, we note that the circularized flow constitutes a magnetic dynamo that greatly amplifies the azimuthal component of the magnetic field. The optically thick emission is dominated by emitting elements on the near and far sides of the black hole, for which the Extraordinary wave has a polarization direction parallel to the reference axis. In the left panel of Figure 17, this optically thick component is indicated by the dashed curve. In contrast, the dominant contribution in the thin region comes from the blue shifted emitter to the side of the black hole, where the Extraordinary wave has a polarization direction mostly perpendicular to this axis. This component is shown as a dotted curve in the left panel of Figure 17.

Another important result of this analysis is that only modest accretion rates appear to be consistent with the polarization characteristics of Sgr A* at mm and sub-mm wavelengths. The emitting region is compact—evidently no larger than a handful of Schwarzschild radii. Yet hydrodynamical simulations suggest a higher rate of capture at larger radii (at $\sim 10^4\ r_s$ or so). If this modeling is correct, this would seem to suggest that $\dot{M}$ is variable, perhaps due to the gradual loss of mass with decreasing radius that we discussed above.

The low value of $\dot{M}$ $(< 10^{16-17}$ g s$^{-1})$ inferred from the polarization studies is significantly smaller than the upper limit already established for this quantity by the X-ray and IR constraints (Quataert, Narayan, & Reid 1999). These authors argue that the combination of a limit on the X-ray bremsstrahlung emissivity at large radii and the IR emissivity from a thick disk at smaller radii, favor an accretion rate no bigger than about $8 \times 10^{-5}\ M_\odot$ yr^{-1}, comparable to the Bondi-Hoyle estimates for the accretion at larger radii (Coker & Melia 1997).

The latest *Chandra* observations reduce the X-ray limited accretion rate considerably since for low accretion rates, the dominant contribution to the $0.5 - 10$ keV flux is self-Comptonization within the radio emitting plasma, rather than bremsstrahlung. The first epoch data show a point source at the location of the central engine with a rather low X-ray luminosity ($\sim [0.5 - 0.9] \times 10^{34}$ erg s^{-1}) in the 0.5-10 keV band (Baganoff et al. 2001). Figure 18 shows the complete spectrum that includes the thermal synchrotron emission in the sub-mm range, together with the self-Comptonized component (Melia, Liu, & Coker 2000). These authors find that a best fit to the Nobeyama and IRAM data alone produces a corresponding X-ray flux that is too high (compared to the *Chandra* measurement) by about a factor of 4, whereas a best fit to the JCMT data produces a self-Comptonized flux that is too low by the same factor. The fit shown in this figure is for the combined sub-mm data sets. (The NTT upper limit is from Menten et al. 1997.) This may be interpreted as an indication of the source variability (in both the sub-mm and X-ray portions of the spectrum) between 1996 and 1999. More specifically, the accretion rate through the inner Keplerian region appears to have decreased by about 15% between the two radio measurements. The implied correlated variability between the sub-mm and X-ray fluxes suggests that future observations with *Chandra* may directly test this basic picture for the sub-mm to X-ray emissivity in Sgr A*.

It is clearly essential to now self-consistently match the conditions within the Keplerian region of the flow with the quasi-spherical infall further out. These calculations are necessary and timely. In particular, it is important to update the early estimates for the frequency-dependent size of Sgr A* (Melia, Jokipii, & Narayanan 1992) in view of the improved restrictions on the properties of the accreting gas. At each frequency, the emission is dominated by the "shell" of gas at which the radiation becomes self-absorbed, thus stratifying the medium. This can provide a powerful tool for testing our understanding of this system with frequency-dependent imaging of the central region.

In summary, the emission in Sgr A* (if produced in the accretion region) requires a very deep potential well, so the case for a massive black hole rather than a distributed dark matter has grown stronger. Whether the radiation mechanism is thermal or non-thermal, the radiative efficiency of the infalling gas must be very low ($< 10^{-5}$). All things considered, this low efficiency is probably due to either a sub-equipartition magnetic field (for either thermal or non-thermal models), or to the separation of the gas into a two-temperature plasma with $T_e \ll T_p$. The current limit on the accreted specific angular momentum appears to be inconsistent with the formation of a large disk, fossil or otherwise (Falcke & Melia 1997), favoring instead the circularization of the infalling plasma when it plum-

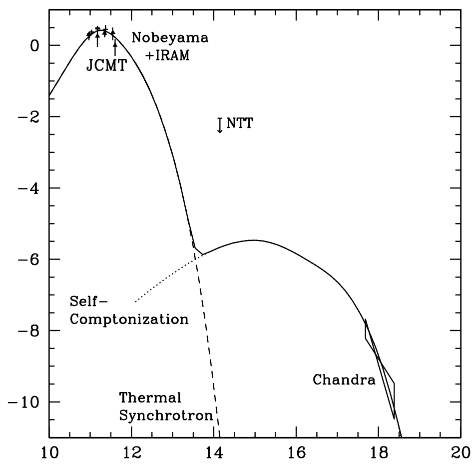

Figure 18 The Comptonized spectrum calculated self-consistently with the best-fit sub-mm model for the combined Nobeyama and IRAM data gathered in October 1996, and the JCMT data gathered in 1999. The inferred accretion rate for this case is 3.5×10^{15} g s^{-1}. The *Chandra* data were obtained with an observation in 1999. Dashed curve: thermal synchrotron; Dotted curve: the self-Comptonized component; Solid curve: the total spectrum. The references for the radio and X-ray data are given in the text. Triangles: JCMT data; Bars: Nobeyama and IRAM data. (From Melia, Liu, & Coker 2000.)

mets to within $50\,r_s$ or so of the black hole. The spectral and polarization data pertaining to the sub-mm bump are consistent with this portion of the spectrum arising from the inner Keplerian flow within $10 - 20\,r_s$ of the accretor.

5.2 Emission due to Non-Accretion Processes

If the dominant emission is not due to the accreting gas one can consider whether the observed spectrum is in fact produced by an outflow or a jet launched from the vicinity of the black hole. The essential element of this model is the ejection of a magnetized plasma containing relativistic electrons or pairs through a nozzle above the event horizon. In this picture, the infalling plasma emits rather weakly but may contribute to the expulsion of matter which is then responsible for the radio and X-ray emission.

In the context of AGNs, Blandford & Königl (1979) proposed that flat-spectrum radio cores are incoherent, nonthermal, synchrotron-emitting jets. Stimulated by this, Reynolds & McKee (1980) first considered the possibility that the flat to inverted radio spectrum of Sgr A* may be due to an analogous jet or wind from a stellar object or a supermassive black hole. They also argued that Sgr A* is unlikely to be gravitationally bound, because its equipartition energy density is too large. The idea was revived by Falcke, Mannheim, & Biermann (1993) who, based on the jet-disk symbiosis idea (Falcke & Biermann 1995; Falcke & Biermann 1999), showed that the basic properties of Sgr A* may be explained by a scaled down AGN-jet model, requiring a very low accretion rate ($\dot{M} \gtrsim 10^{(-8)-(-7)} M_\odot$ yr^{-1}) to power the outflow.

Possible launching mechanisms for the jets have been discussed in the literature (e.g., Appl & Camenzind 1993; Koide et al. 2000) and usually invoke pressure and magnetohydrodynamic acceleration of plasma from the inner edge of an accretion flow. This acceleration region close to the black hole, summarily called a "nozzle", should radiate at the highest synchrotron frequencies, i.e., in the sub-mm regime for Sgr A*. However, as realized by Duschl & Lesch (1994), the steep cut-off towards the IR in the Sgr A* spectrum requires a rather narrow energy distribution for electrons, i.e., a quasi-monoenergetic population. Such a distribution is consistent with a Maxwellian, which was shown earlier to result in a transparent medium (i.e., a sharp drop-off in flux) above $\sim (2-3)\times10^{11}$ Hz (Melia 1992; Melia 1994). Self-absorption, on the other hand will occur somewhere in the mm-wave regime and thus, together with the peaked electron distribution, produces a peaked spectrum (Falcke 1996b; Beckert & Duschl 1997).

To capture the basic elements of this picture, we may consider a simple toy model with four parameters: the magnetic field B, the electron density n, the electron Lorentz factor $\gamma_{\rm e}$, and the volume $V = 4/3\,\pi R^3$, using for simplicity a one-temperature (i.e., a quasi mono-energetic) electron distribution, with the distance being set to 8.5 kpc. On the observational side we have three measurable input parameters: the peak frequency $\nu_{\rm max} \sim \nu_{\rm c}/3.5$ of the synchrotron spectrum (characteristic frequency $\nu_{\rm c}$), the peak flux $S_{\nu_{\rm max}}$, and the low-frequency turnover of the sub-mm bump at the self-absorption frequency $\nu_{\rm ssa}$. A fourth parameter can be gained if one assumes that the magnetic field and relativistic electrons are in approximate equipartition, i.e. $B^2/8\pi = k^{-1} n_{\rm e}\gamma_{\rm e} m_{\rm e} c^2$ with $k \sim 1$. With this condition one obtains from synchrotron theory that

$$\gamma_{\rm e} = 118\; k^{2/7} \left(\frac{\nu_{\rm max}}{\rm THz}\right)^{5/17} \left(\frac{\nu_{\rm ssa}}{\rm 100GHz}\right)^{-5/17} \left(\frac{F_{\nu_{\rm max}}}{\rm 3.5Jy}\right)^{1/17}, \tag{4}$$

$$B = 75\,{\rm G}\; k^{-4/17} \left(\frac{\nu_{\rm max}}{\rm THz}\right)^{7/17} \left(\frac{\nu_{\rm ssa}}{\rm 100GHz}\right)^{10/17} \left(\frac{F_{\nu_{\rm max}}}{\rm 3.5Jy}\right)^{-2/17}, \tag{5}$$

$$n_{\rm e} = 2\times10^{6}{\rm cm}^3\; k^{7/17} \left(\frac{\nu_{\rm max}}{\rm THz}\right)^{9/17} \left(\frac{\nu_{\rm ssa}}{\rm 100GHz}\right)^{25/17} \left(\frac{F_{\nu_{\rm max}}}{\rm 3.5Jy}\right)^{5/17}, \tag{6}$$

$$R = 1.5\times10^{12}{\rm cm}\; k^{-1/17} \left(\frac{\nu_{\rm max}}{\rm THz}\right)^{-16/51} \left(\frac{\nu_{\rm ssa}}{\rm 100GHz}\right)^{-35/51} \left(\frac{F_{\nu_{\rm max}}}{\rm 3.5Jy}\right)^{8/17} \tag{7}$$

Apparently the parameter k enters only weakly and hence the above values should reflect the characteristic properties of the sub-mm emission region in Sgr A* to within a factor of a few. The electron Lorentz factor corresponds to around 2×10^{11} K using $\gamma_{\rm e} \sim \sqrt{12}k_{\rm b}T_{\rm e}(m_{\rm e}c^2)^{-1}$ the average Lorentz factor for a relativistic Maxwellian (see § 5.1). The size R corresponds to $\sim$ 2 Schwarzschild radii and is consistent with the sub-mm bump coming from the direct vicinity of the black hole.

If these parameters describe the nozzle of a jet, rather than a static corona as proposed by (Beckert & Duschl 1997), the emission at lower frequencies can be obtained in a straight forward manner by following the evolution of the plasma on its way out using the Euler equation. In the supersonic, post-nozzle regime the jet mainly accelerates through its longitudinal pressure gradient to bulk Lorentz factors around $\gamma_{\rm j} = 2-3$. As the plasma moves outwards and expands, roughly filling a conical jet with $B \sim r^{-1}$ and $n \sim r^{-2}$, the peak synchrotron frequency will drop continuously. Integration over the entire length of the jet, taking into account the changing Doppler factor and adiabatic losses yields a slightly inverted

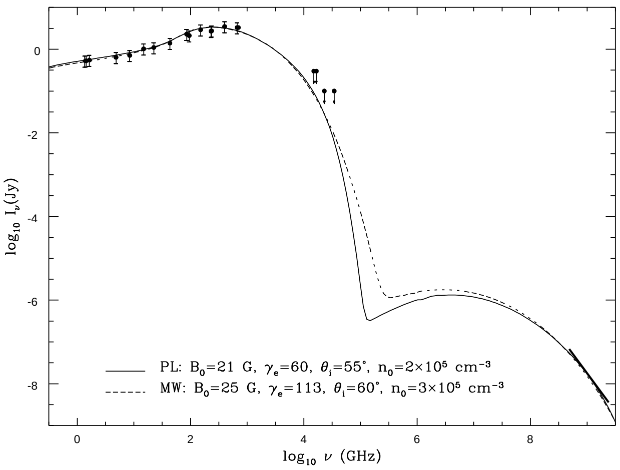

Figure 19 Broad-band spectrum of Sgr A* produced by a jet model, with a power-law electron distribution (PL) and a relativistic Maxwellian (MW). The width of the nozzle is $r_0 = 4\,r_s$ and $r_0 = 3r_s$, respectively, while its height is at $z_0 = 3r_0$. The data are from Fig. 10, augmented by the high-frequency measurements discussed in Serabyn et al. (1997). The *Chandra* data are also shown. (From Falcke & Markoff 2000.)

radio spectrum (Falcke 1996a) with $\alpha \simeq 0 - 0.25$ as a function of the inclination angle.

Falcke & Markoff (2000) have carried out these calculations for arbitrary electron energy distributions. Figure 19 shows the results for a Maxwellian and a curtailed power-law distribution. The model can account for the cm to sub-mm spectrum. Moreover, when one calculates synchrotron radiation from the relativistic electrons, one also has to take into account that the very same electrons will up-scatter their own synchrotron photons via the synchrotron self-Compton process (SSC), as was the case for the infall model (see § 5.1). Since the SSC emission is proportional to $n_{\rm e}^2$ the emission is dominated by the most compact region, in this case, the sub-mm bump or the nozzle. For electron Lorentz factors $\gamma_{\rm e} \sim 10^2$ the scattered sub-mm emission should then appear at very soft X-rays. Indeed, for Sgr A* the SSC component appears as a second bump in Figure 19, accounting for the low and very soft X-ray emission detected by Chandra (Baganoff et al. 2001). If this interpretation is correct one would expect to see correlated variability between sub-mm and X-ray emission, though it is not yet clear how the variability amplitudes compare with those of the accretion model (see Fig. 18).

As is the case in any stratified emission model, the radiation from the jet at different frequencies will be dominated by different regions where the optical depth τ approaches unity. This yields roughly a $\nu^{-0.9}$ dependence of the characteristic size of the emission region as seen for example in extragalactic sources like M81* (Bietenholz, Bartel, & Rupen 2000). This also predicts a frequency-dependent core-shift which should be observable with VLBI phase-referencing observations. The peaked electron distribution and the absence of a power-law at high frequencies in Sgr A* also imply that the emission at one observing frequency is very compact highlighting only a narrow section of the jet. This is consistent with current VLBI observations.

The narrow electron distribution needed in Sgr A* is rather unusual and may indicate the absence of shocks along the jet commonly found in more luminous AGNs. If the jet is launched from a two-temperature plasma, the electrons would not be hot enough while the protons could reach temperatures in excess of 10^{12} K at the inner edge as a function of black hole spin (Manmoto 2000). At this temperature proton-proton collisions will become inelastic and lead to the production of pions with a subsequent decay into neutrinos, γ-rays, and enough energetic pairs with $\gamma_{\rm e} \simeq 60$ to account for the jet emission (Markoff, Falcke, & Biermann 2000). The jet plasma in such a model would then be a mixture of "cold" electrons and "hot" pairs. If the number of cold electrons from the normal plasma dominates, this in itself could lead to substantial depolarization of linear polarization and conversion to circular polarization (Bower, Falcke, & Backer 1999; Beckert & Falcke 2001).

In future work, it will be necessary to understand how the jet, if present, is coupled to the inflowing plasma (see, e.g., Yuan 2000). Is the accreting gas responsible for producing it, or is the jet simply a by-product of a spinning black hole? And in either case, if we're seeing emission from a jet in Sgr A*, why is the accreting plasma so underluminous?

This latter condition is also a necessary feature in models that invoke static configurations of hot gas. Duschl & Lesch (1994) and Beckert & Duschl (1997) explain the radio to FIR-spectrum of Sgr A* as incoherent, optically thin synchrotron radiation from relativistic electrons (and/or positrons) bound to the central gravitational potential. If the spectrum is treated in a time-averaged fashion (so that it has a dependence $\sim \nu^{1/3}$ between 1 and 10^3 GHz) the required particle distribution is quasi-mono energetic with $\Delta E/E < 7$ (E being the characteristic electron energy and ΔE the width of its distribution). Beckert & Duschl (1999) consider relativistic thermal distributions as a natural subclass and an acceptable fit to the time averaged spectrum. Acceleration processes that may lead to such quasi-monoenergetic distributions of electron energies are discussed by Duschl & Jauch (2000).

In this picture, Sgr A* is modeled as a core-shell structure with two homogeneous components. The core with an electron temperature of $T_e = 5 \times 10^{11}$ K and a magnetic field of $B = 70$ G is only marginally larger than the Schwarzschild radius, and is visible only as the sub-mm excess flux. In a variation of this basic model, Beckert & Duschl (1999) discuss a core component made up of the central regions of an ADAF disk. The much more extended shell is optically thin above ≈ 2 GHz and is filled with electrons of $T_e = 2 \times 10^{12}$ K in a 2 G magnetic field. The self-Comptonization of synchrotron photons by the relativistic electrons is minimal due to the small Thomson optical depth of $\tau \approx 10^{-2}$ and appears in the UV and soft X-rays. The corresponding flux can be matched to the *Chandra* measurement, but the spectral shape in X-rays depends strongly on the column density of absorbing material and the electron temperature in the core component.

Future work with this model will need to address issues such as (1) how does the static configuration account for the *instantaneous* spectrum of Sgr A*? (2) what determines the temperature and magnetic field of the plasma? (3) what are the implied polarization properties of this gas? and (4) what produces the variability at radio frequencies? It now appears that some of the short-term variability in Sgr A* is indeed intrinsic to the source and a variable spectral index appears to be incompatible with a one- or two-component model.

In conclusion, we can say that, while the underlying concepts for the various emission models of Sgr A* sound rather different, physical quantities such as B, the particle density, and the temperature and/or particle Lorentz factor, have values that are slowly converging with one another. This is due primarily to the ever improving observational constraints and it is expected that the current degeneracy of models may collapse to a unified picture involving some of the ideas discussed in these sections.

5.3 Alternatives to the Black Hole Paradigm

Alternatives to a supermassive black hole as the central dark mass concentration have so far tended to concentrate on the structure of the central object, rather than its emissivity. Nonetheless, the current observational limits inferred from Sgr A*'s spectrum do tightly constrain (or even exclude) some of them. However, until definitive proof of an event horizon has been obtained (see § 6), other possibilities must remain open—indeed should continue to be explored.

One idea that has been explored recently is that of a nonbaryonic ball comprised of degenerate, self-gravitating heavy neutrino matter (Tsiklauri & Viollier 1998). Its size is a strong function of the neutrino mass m_ν. This scenario requires us to postulate the existence of as yet unidentified neutrinos with mass > 17 keV, which would condense into a sphere with a characteristic size of about 0.01 pc. However, to explain even more massive dark compact objects, such as that in M87 with $10^9\,M_\odot$, the putative neutrino mass cannot be greater than 17 keV, for otherwise the neutrino ball itself attains an event horizon. Given that the new stellar orbits determined by Ghez, Morris, & Becklin (2000) at the Galactic Center limit the volume of the region within which the dark matter is contained even further, the neutrino mass would now need to be substantially greater than this limit.

It thus appears that a black hole-free universe probably cannot be constructed in this way, but let us suppose that Sgr A* is a neutrino ball. Its luminosity in that case would be due to disk emission from gas spiraling through the gravitational potential of a radially-dependent enclosed mass. Thus, at any given radius, the dissipation rate falls below the corresponding value for the case where all the mass is concentrated at a central point. This introduces the attractive feature of accounting for a decreasing radiative efficiency as the gas approaches the middle. However, it also begs the question of what happens to the infalling matter. Presumably, it stays trapped within the neutrino ball, but over the age of the Galaxy, some $10^6\,M_\odot$ of plasma will have condensed to the bottom of the potential well, assuming that Bondi-Hoyle accretion proceeds at the rate suggested by the large scale simulations (see above). In a sense, this defeats the purpose of having a ball of degenerate neutrinos.

Of course, one could consider other particles to reconstruct the dark compact mass at the Galactic Center. Instead of fermions, one could try bosons, such as Higgs particles, and postulate a massive boson star, perhaps due to topological defects in the cosmological evolution (Torres, Capozziello, & Lambiase 2000). However, at this writing, these models remain very speculative and no clear bound on the required particle mass can be given. On the other hand, supermassive stars of ordinary matter with an even heavier accretion disk (Kundt 1990) can already be comfortably ruled out, based on the low near-infrared flux at the position of Sgr A*. Finally, suggestions that Sgr A* could be a matter-creating "white hole" (Burbidge & Hoyle 1996) or an accreting "near-black-hole" need to be fleshed out with more detail, commensurate with the richness of the current database for this object.

6 STRONG GRAVITY EFFECTS

The ever growing interest in Sgr A* has already yielded a number of tantalizing results, the most important being that Sgr A* is the best supermassive black hole candidate we know. Beyond trying to model the emission from this source, it is worth thinking about the possibility of utilizing its relative proximity in order to test the predictions of General Relativity in the strong field limit. For example, the fact that Sgr A*'s mass is known so precisely and that the emitting gas is apparently becoming transparent at mm to sub-mm wavelengths near the marginally-stable orbit, means that timing studies of this source with bolometric detectors on single-dish telescopes may reveal the black hole's spin (Melia et al. 2001). Surprising as this may seem, we are at the stage where we can begin to ask questions such as "Is there really an event horizon in this source?" Embedded within a bright star cluster, Sgr A* might also be a microlens, producing effects that will be measurable with our ever improving spatial resolution of this region.

6.1 Imaging the Event Horizon

The VLBI resolution is rapidly approaching a scale commensurate with the actual size of Sgr A*'s event horizon. When we realize that the presence of the sub-mm bump in the spectrum is indicative of a compact emission region a mere couple of Schwarzschild radii in size, it becomes worthwhile exploring the possibility of actually "seeing" the shadow of the black hole using VLBI imaging techniques. This naturally will have to be done at the highest radio frequencies where the resolution is the best, and the scatter-broadening of Sgr A* by the intervening medium is the lowest.

At sub-mm wavelengths, the synchrotron emission is not self-absorbed (Melia 1992; Melia 1994; Falcke 1996b); the medium's transparency at the shortest wavelengths allows us to view the emitting gas all the way down to the event horizon, whose size is $(1+\sqrt{1-a_*^2})r_s/2$, where $r_s \equiv 2GM/c^2$, M is the mass of the black hole, G is Newton's constant, c the speed of light, $a_* \equiv Jc/(GM^2)$ is the dimensionless spin of the black hole in the range 0 to 1, and J is the angular momentum of the black hole. Bardeen (1973) described the idealized appearance of a Schwarzschild black hole *in front* of a planar emitting source (e.g., a star), showing that it literally would appear as a "black hole" of diameter $\sqrt{27}r_s/2$. At that time, such a calculation was of mere theoretical (rather than practical) interest. To further check whether there is indeed a realistic chance of seeing this "black hole" in the Galactic Center, Falcke, Melia, & Agol (2000) simulated the appearance of the emitting gas *surrounding* Sgr A* using a general relativistic (GR) ray-tracing code for various combinations of black hole spin, inclination angle, and morphology of the surrounding emission region. The simulations take the scatter broadening and the instrumental resolution of VLBI at sub-mm waves into account.

As revealed by these calculations the presence of an event horizon inside a transparent radiating source will naturally lead to a deficit of photons in the center, called a "shadow" by Falcke, Melia, & Agol (2000) and independently de Vries (2000). The size of the shadow is larger than the event horizon due to the strong bending of light by the black hole and is of order $5r_s$ in diameter.

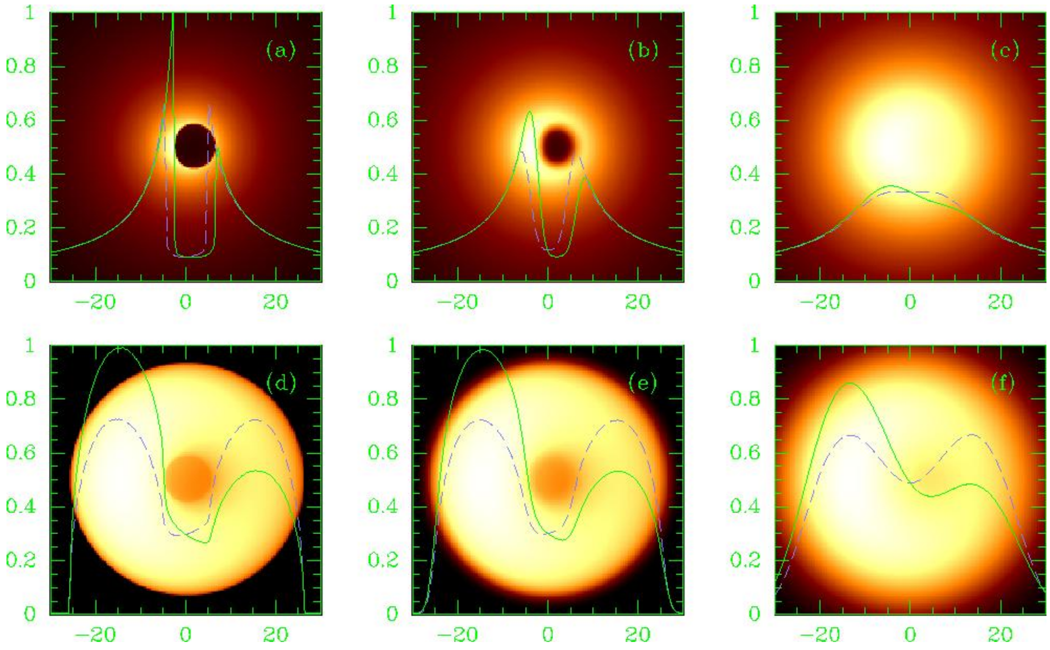

Figure 20 An image of an optically thin emission region surrounding a black hole with the characteristics of Sgr A* at the Galactic Center. The black hole is here either maximally rotating ($a_* = 0.998$, panels a-c) or non-rotating ($a_* = 0$, panels d-f). The emitting gas is assumed to be in free fall with an emissivity $\propto r^{-2}$ (panels a-c) or on Keplerian shells (panels d-f) with a uniform emissivity (viewing angle $i = 45°$). Panels a&d show the GR ray-tracing calculations, panels b&e are the images seen by an idealized VLBI array at 0.6 mm wavelength taking interstellar scattering into account, and panels c&f are those for a wavelength of 1.3 mm. The intensity variations along the x-axis (solid green curve) and the y-axis (dashed purple/blue curve) are overlayed. The vertical axes show the intensity of the curves in arbitrary units and the horizontal axes show the distance from the black hole in units of $r_s/2$ which for Sgr A* is 3.9×10^{11} cm ~ 3 μas. (From Falcke, Melia & Agol 2000.)

Two disparate cases are reproduced here (see Fig. 20), which include a rotating and a non-rotating black hole, a rotating and an inflowing emission region, as well as a centrally peaked and a uniform emissivity.

The shadow can be clearly seen with a diameter of $4.6\,r_s$ (30 μas) in diameter for the rotating black hole and with a radius of $5.2\,r_s$ (33 μas) for the non-rotating case. The emission can be asymmetric due to Doppler shifts associated with rapid rotation (or inflow/outflow) near the black hole. The size of this shadow is within less than a factor of two of the maximum resolution already achieved by sub-mm VLBI ($\sim 50\mu$as, Rantakyro et al. 1998). It may also be feasible to do polarimetric imaging at mm and sub-mm wavelengths, which would reveal additional effects of strong gravity distortions (Bromley, Melia, & Liu 2001).

Interestingly, the scattering size of Sgr A* and the resolution of global VLBI arrays become comparable to the size of the shadow at a wavelength of about 1.3 mm. As one can see from Figure 20, the shadow is still almost completely washed out for VLBI observations at 1.3 mm, while it is very apparent at a factor two shorter wavelength (Figs. 20 b&e). In fact, already at 0.8 mm (not shown here) the shadow can be seen easily. Under certain conditions, i.e., a very homogeneous emitting region, the shadow would be visible even at 1.3 mm. The technical methods to achieve such a resolution at wavelengths shorter than 1.3 mm are currently being developed and a first detection of Sgr A* at 1.4 mm with VLBI has already been reported (Krichbaum et al. 1998). Pushing the VLBI technology even further, towards λ0.8 or even λ0.6 mm, should eventually provide the first direct evidence for the existence of an event horizon. Alternatively one could think of space-based X-ray imaging of this shadow as has been proposed recently (Cash et al. 2000). However, this technology is still far in the future and Sgr A* is rather weak in X-rays.

The imaging of this shadow would confirm the widely held belief that most of the dark mass concentration in the nuclei of galaxies such as ours is contained within a single object. A non-detection with sufficiently developed techniques, on the other hand, might pose a major problem for the standard black hole paradigm. Because of this fundamental importance, this experiment should be a major motivation for intensifying the current development of sub-mm astronomy in general and mm- and sub-mm VLBI in particular.

6.2 Interactions of Sgr A with the Central Star Cluster*

Besides gravitational light bending very close the event horizon, one might also expect to see microlensing of stars by Sgr A*. When a star passes behind Sgr A*, we would expect to see a temporary amplification of its luminosity. These events occur with a rate that depends strongly on the assumed stellar distribution in the Galactic Center and in the Galactic plane. Current estimates predict about 10^{-3} events per year for amplifications lasting one year down to a detection limit of 17 mag in K (Alexander & Sternberg 1999). For current telescopes and monitoring programs, the detectability of this effect is rather low. However, the probability of *microlensing* the background stars is in fact increased by the combined action of a central black hole and the dense central star cluster. Depending on the stellar background density, this effect could provide a 1% probability of seeing a microlensing effect in the inner $2''$at the Galactic Center at any given time (Alexander & Loeb 2001). This is because the Einstein radius of Sgr A* for a source at infinity is rather large, i.e., about $1\overset{''}{.}75$. Since lensed images of a star on the opposite side of a black hole should be lined up with the black hole itself, one can try to use current NIR maps to look for such a correlation in a statistical way. Using this method, Alexander (2001) finds further evidence for Sgr A* being coincident with the center of gravity in the Galactic nucleus.

Another impact Sgr A* may have on the surrounding stars is the tidal disruption of cluster members when they venture too close to the black hole (Rees 1982; Khokhlov & Melia 1996). Again, the actual event rate depends on the exact stellar density, but is expected to be around several times 10^{-5} yr^{-1} (Alexander 1999). While it is unlikely for us to directly witness such an event, its remnant could still be visible today. In this regard, the inferred age of Sgr A East, its morphology, and energetics would fit such a scenario (Khokhlov & Melia 1996). In addition the yet unidentified fossil remains of previous explosions might also be visible in low-frequency observations of the Galactic Center (Kassim et al. 1999) and in the distribution of electron-positron annihilation radiation from the central bulge (Fatuzzo, Melia, & Rafelski 2001).

While some of these arguments offer supportive, rather than direct, evidence for the existence of the black hole, future determinations of the stellar orbits at the Galactic Center using space interferometry (e.g., with *DARWIN*; Wilson

2000) promise much more insight. These orbits may not help us to distinguish between rotating and non-rotating black holes, but they will clearly differentiate between point and extended mass distributions (Munyaneza, Tsiklauri, & Viollier 1999).

7 SGR A* AS A MODEL FOR AGN ACTIVITY

The prospects for applying what we are learning in the Galactic Center to the broader study of Active Galactic Nuclei (AGNs) are quite promising. We mention only a few areas of overlap here, but the cross-fertilization is likely to blossom quickly into the future. The recent work on the gas dynamics in the Galactic Center has greatly improved our understanding of the gaseous flows surrounding a massive black hole, particularly with regard to properties such as the specific angular momentum distribution, density, and temperature of the inflowing plasma. With the appropriate extrapolation of the physical conditions, this information can be valuable in trying to determine the origin of the Broad Line Region (BLR) in AGNs. On larger scales, we see the importance and action of magnetic fields. While our view is still patchy, we have observed toroidal magnetic fields in molecular clouds (Novak 1999) accreting towards the center (von Linden et al. 1993) and interacting with the large scale poloidal field seen in the filaments (Morris 1994; Chandran, Cowley, & Morris 2000).

The molecular clouds, especially the circumnuclear disk (CND), could be the Galactic Center's version of the obscuring torus inferred for many AGNs (Antonucci 1993). The CND/torus might simply be the remnant of tidally disrupted clouds (Sanders 1999) trapped in the transition region where the black hole mass starts to dominate the gravitational potential (Duschl 1989).

Further in we see what could be considered the Narrow-Line-Region of AGNs: the gas streamers and colliding stellar winds. The hot gas in the minispiral is a strong emitter of narrow Hα (see the NICMOS Pa α image in Fig. 3) and similarly narrow (in AGN terms) emission lines are produced by the stellar winds from luminous stars in the center. Currently, the excitation of this gas is only due to stars and would at best resemble an H II galaxy (Shields & Ferland 1994), as found in our cosmic neighborhood (Ho, Filippenko, & Sargent 1997). However, with a velocity dispersion of several hundred km s^{-1} this gas would immediately turn into a typical NLR should Sgr A* light up in the future. The presence of so much gas near the black hole suggests that sooner or later the accretion onto Sgr A* might become much higher. We may have already undergone the first stage of this accretion event in the form of a star burst several million years ago, producing today's young and hot stars in the central parsecs. Morris, Ghez, & Becklin (1999) have argued on this basis that the Galactic Center may be exhibiting a limit cycle of recurrent nuclear activity, with a timescale ($\sim 10^7$ yrs) dictated by the evolution of the most massive stars. This highlights the starburst-AGN connection.

So far we have not seen any evidence for a broad line region near Sgr A*. The spectra of many AGNs, including Seyfert galaxies and quasars, are distinguished by strong, broad emission lines, with a full width at half maximum intensity (FWHM) of $\sim 5,000$ km s^{-1}, and a full width at zero intensity (FWZI) of $\sim 20,000$ km s^{-1} (e.g., Peterson 1997). From the observed strength of UV emission lines, we know that the temperature of the emitting plasma is on the order of a few times 10^4 K (e.g., Osterbrock 1989), insufficient to produce the observed line widths via thermal (Doppler) broadening. Instead, bulk motions of the BLR gases appear to be responsible for the line broadening.

In AGNs, the BLR gases have apparently condensed into clouds, but the medium surrounding Sgr A* does not share this property. Fromerth & Melia (2001) have explored various scenarios for the AGN cloud formation based on the underlying principle that the source of plasma is ultimately that portion of the gas trapped by the central black hole from the interstellar medium. Winds accreting onto a central black hole are subjected to several disturbances capable of producing shocks, including a Bondi-Hoyle flow, stellar wind-wind collisions, and turbulence. Shocked gas is initially compressed and heated out of thermal equilibrium with the ambient radiation field; a cooling instability sets in as the gas is cooled via inverse-Compton and bremsstrahlung processes. If the cooling time is less than the dynamical flow time through the shock region, the gas may clump to form the clouds responsible for broad line emission seen in many AGN spectra. In the case of Sgr A*, this time differential does not appear to be sufficient for the cloud condensation to occur in the gravitationally trapped gas. For AGNs, however, the preliminary calculations in this study suggest that clouds form readily. Their distribution agrees with the results of reverberation studies, in which it is seen that the central line peak (due to infalling gas at large radii) responds slower to continuum changes than the line wings, which originate in the faster moving, circularized clouds at smaller radii. Very interestingly, it appears that the required cloud formation is one in which ambient gas surrounding the black hole (e.g., from stellar winds) is captured gravitationally and begins its infall with a (specific angular momentum) λ representative of a flow produced by many wind-wind collisions and turbulence (see Fig. 14) rather than a smooth Bondi-Hoyle bow shock. In this process, the gas eventually circularizes at $r_{circ} \approx 2\lambda^2 r_s$ (see § 4), but by that time all of the BLR clouds have been produced, since at that radius the gas presumably settles onto a planar disk. As such, this picture is distinctly different from "conventional" models in which the clouds are produced within a disk and are then accelerated outwards by such means as radiation pressure or magnetic stresses.

Finally, the radio emitting region surrounding the black hole in the Galactic Center may be similar to what we see in the cores of more luminous AGNs. In all classes of accreting black holes, a fraction of sources produce flat-spectrum radio cores. In quasars they have been studied with VLBI and have been resolved into relativistic jets (Zensus 1997). We have not yet seen a jet in Sgr A*, and its existence would be irrelevant to Sgr A*'s spectrum if the emission is dominated by the accreting gas. It is interesting to note that the spiral galaxy M81 has a radio core with properties not unlike those of Sgr A*. This source has been observed with VLBI and was recently resolved into an extremely compact, though stretched out, structure (Bietenholz, Bartel, & Rupen 2000). It has a similar, unusually high circular-to-linear polarization ratio as Sgr A* (Brunthaler et al. 2001). The extended emission in this source on scales of $\sim 10 - 100$ mas is less than 6% of the total flux density. The size and orientation of this structure are frequency dependent, bending from $\sim 40^\circ$ at 22 GHz to $\sim 75^\circ$ at 2.3 GHz. These characteristics still leaves the question open as to whether the dominant emitting region is inflowing or outflowing on a compact scale. We may be seeing a combined core-jet emitter, in which the outflow contributes at least partially to the overall flux. In general, Sgr A*-like radio cores seem to be rather common in nearby galaxies with a low level of nuclear activity (see, e.g., Wrobel & Heeschen 1984; Nagar et al. 2000; Falcke et al. 2000), indicating that Sgr A* can tell us a great deal about the active nuclei of other galaxies.

8 CONCLUSIONS

We have learned a great deal about the principal interactions within the inner few parsecs at the Galactic Center, but as is often the case, important questions arise with each uncovering of a new layer. There is no longer any doubt that a significant concentration of dark matter occupies the region bounded by the inner 0.015 pc. This size is sufficiently small that we can rule out distributions of stellar-sized objects, such as neutron stars or brown dwarfs as the constituents. Such a distribution would need to be highly peaked in the center, and therefore considerably out of equilibrium (Genzel et al. 1997). Its lifetime would be of order 10^7 years, much smaller than the age of the galaxy (Maoz 1998), leaving us to ponder why we are viewing this region at such a special time. That there is a massive point-like object in the middle is now hard to dispute. It doesn't move relative to objects around it, and it has a spectrum like no other in the Milky Way, though it shares many characteristics in common with the cores of other nearby galaxies.

One of the principal problems now facing us is to understand how in fact Sgr A* produces its spectrum. The Galactic Center is rich in gas, and some of it must be funneling into the black hole. Yet this process does not appear to be converting very much kinetic and gravitational energy into radiation, making Sgr A* extremely sub-Eddington. This departure from our naive expectations is forcing us to rethink the basic elements of accretion physics. So theorists are now grappling with questions such as (1) is the inflow advection dominated, carrying most of its energy through the event horizon? (2) is the assumption of equipartition between the magnetic field and the gas an over-simplification that leads to a great overestimation of the magnetic field intensity, and hence of the synchrotron emissivity? (3) does the plasma separate into two temperatures as it gets compressed and heated? and (4) does the black hole and/or the infalling plasma produce a jet at small radii that then dominates the emissivity from this source? Ongoing polarimetric observations at mm and sub-mm wavelengths will greatly assist in this endeavor, providing the necessary constraints that are complementary to those implied by the spectroscopic measurements.

Perhaps one of the most exciting developments in this program will be the imaging of Sgr A*'s shadow against the backdrop of optically thin emitting plasma at sub-mm wavelengths within the next 5 to 10 years. The appearance of this shadow is a firm prediction of General Relativity, which mandates a unique shape and size for the region where light bending and capture are important. There has never been such an opportunity to place the existence of black holes on such a firm footing. Galactic black hole binaries contain compact objects that are too small, and the cores of other galaxies are simply too far away. Sgr A* at the Galactic Center has a size that is now on the verge of detectability with sub-mm VLBI. This coming decade may finally give us a view into one of the most important and intriguing predictions of General Relativity.

Acknowledgments

The authors are indebted to the vibrant Galactic Center community for the many discussions and opportunities to learn about the latest developments in this exciting field. They are particularly grateful to Don Backer, Geoff Bower, Dan Gezari, Mark Morris and Charles Townes for carefully reading through the text and making helpful suggestions. This work was supported by a Sir Thomas Lyle Fellowship and a Miegunyah Fellowship for distinguished overseas visitors at the University of Melbourne, and by NASA grants NAG5-8239 and NAG5-9205 at the University of Arizona.

REFERENCES

Agol, E. 2000, ApJ, 538, L121

Aitken, D. K., Greaves, J., Chrysostomou, A., Jenness, T., Holland, W., Hough, J. H., Pierce-Price, D., & Richer, J. 2000, ApJ, 534, L173

Aitken, D. K., Smith, C. H., Gezari, D., McCaughrean, M., & Roche, P. F. 1991, ApJ, 380, 419

Aitken, D. K., Smith, C. H., Moore, T. J. T., & Roche, P. F. 1998, MNRAS, 299, 743

Alexander, T. 1999, ApJ, 527, 835

Alexander, T., & Loeb, A. 2001, ApJ, 551, 223

Alexander, T., & Sternberg, A. 1999, ApJ, 520, 137

Antonucci, R. 1993, ARA&A, 31, 473

Appl, S., & Camenzind, M. 1993, A&A, 274, 699

Backer, D. C. 1996, in IAU Symp. 169: Unsolved Problems of the Milky Way, Vol. 169, 193

Backer, D. C., & Sramek, R. A. 1999, ApJ, 524, 805

Backer, D. C., Zensus, J. A., Kellermann, K. I., Reid, M., Moran, J. M., & Lo, K. Y. 1993, Science, 262, 1414

Baganoff, F., Bautz, M., Brandt, N., Cui, W., Doty, J., Feigelson, E., Garmire, G., Maeda, Y., Morris, M., Pravdo, S., Ricker, G., & Townsley, L. 2001, ApJ, submitted

Balick, B., & Brown, R. L. 1974, ApJ, 194, 265

Bally, J., & Yusef-Zadeh, F. 1989, ApJ, 336, 173

Bardeen, J. M. 1973, in Black Holes, ed. C. DeWitt & B. S. DeWitt (New York: Gordon & Breach), 215

Beckert, T., & Duschl, W. J. 1997, A&A, 328, 95

Beckert, T., & Duschl, W. J. 1999, in ASP Conf. Ser. 186: The Central Parsecs of the Galaxy, ed. H. Falcke, A. Cotera, W. J. Duschl, F. Melia, & M.J. Rieke (San Francisco: Astronomical Society of the Pacific), 138

Beckert, T., & Falcke, H. 2001, A&A, to be submitted

Becklin, E. E., Gatley, I., & Werner, M. W. 1982, ApJ, 258, 135

Bietenholz, M. F., Bartel, N., & Rupen, M. P. 2000, ApJ, 532, 895

Blandford, R. D., & Begelman, M. C. 1999, MNRAS, 303, L1

Blandford, R. D., & Königl, A. 1979, ApJ, 232, 34

Bondi, H., & Hoyle, F. 1944, MNRAS, 104, 273

Bower, G. C. 2000, GCNEWS, 11, 4

Bower, G. C., & Backer, D. C. 1998, ApJ, 496, L97

Bower, G. C., Backer, D. C., Zhao, J. H., Goss, M., & Falcke, H. 1999a, ApJ, 521, 582

Bower, G. C., Falcke, H., & Backer, D. C. 1999, ApJ, 523, L29

Bower, G. C., Falcke, H., Backer, D. C., & Wright, M. 1999b, in ASP Conf. Ser. 186: The Central Parsecs of the Galaxy, ed. H. Falcke, A. Cotera, W. J. Duschl, F. Melia, & M.J. Rieke (San Francisco: Astronomical Society of the Pacific), 80

Bower, G. C., Falcke, H., Sault, R. J., & Backer, D. C. 2000a, ApJ, to be submitted

Bower, G. C., Wright, M. C. H., Backer, D. C., & Falcke, H. 1999c, ApJ, 527, 851

Bower, G. C., Wright, M. C. H., Falcke, H., & Backer, D. C. 2000b, ApJ, submitted

Bromley, B. C., Melia, F., & Liu, S. 2001, ApJ, in press

Brown, R. L. 1982, ApJ, 262, 110

Brown, R. L., Johnston, K. J., & Lo, K. Y. 1981, ApJ, 250, 155

Brown, R. L., & Lo, K. Y. 1982, ApJ, 253, 108

Brunthaler, A., Bower, G. C., Falcke, H., & Melon, R. R. 2001, ApJ, submitted

Burbidge, G., & Hoyle, F. 1996, in ASP Conf. Ser., Vol. 102, The Galactic Center, ed. R. Gredel (San Francisco: Astronomical Society of the Pacific)

Cash, W., Shipley, A., Osterman, S., & Jay, M. 2000, Nature, 407, 160

Chan, K., Moseley, S. H., Casey, S., Harrington, J. P., Dwek, E., Loewenstein, R., Varosi, F., & Glaccum, W. 1997, ApJ, 483, 798

Chandran, B. D. G., Cowley, S. C., & Morris, M. 2000, ApJ, 528, 723

Coker, R. F., & Melia, F. 1997, ApJ, 488, L149

Coker, R. F., & Melia, F. 2000, ApJ, 534, 723

Cotera, A., Morris, M., Ghez, A. M., Becklin, E. E., Tanner, A. M., Werner, M. W., & Stolovy, S. R. 1999, in ASP Conf. Ser. 186: The Central Parsecs of the Galaxy, ed. H. Falcke, A. Cotera, W. J. Duschl, F. Melia, & M.J. Rieke (San Francisco: Astronomical Society of the Pacific), 240

Davidson, J. A., Werner, M. W., Wu, X., Lester, D. F., Harvey, P. M., Joy, M., & Morris, M. 1992, ApJ, 387, 189

Davies, R. D., Walsh, D., & Booth, R. S. 1976, MNRAS, 177, 319

de Vries, A. 2000, Class. Quantum Grav., 17, 123

Di Matteo, T., Fabian, A. C., Rees, M. J., Carilli, C. L., & Ivison, R. J. 1999, MNRAS, 305, 492

Doeleman, S., Rogers, A. E. E., Backer, D. C., Wright, M., & Bower, G. C. 1999, in ASP Conf. Ser. 186: The Central Parsecs of the Galaxy, ed. H. Falcke, A. Cotera, W. Duschl, F. Melia, & M. J. Rieke (San Francisco: Astronomical Society of the Pacific), 98

Doeleman, S. S., Shen, Z. ., Rogers, A. E. E., Bower, G. C., Wright, M. C. H., Zhao, J. H., Backer, D. C., Crowley, J. W., Freund, R. W., Ho, P. T. P., Lo, K. Y., & Woody, D. P. 2001, AJ, 121, 2610

Duschl, W. J. 1989, MNRAS, 240, 219

Duschl, W. J., & Jauch, Z. 2000, A&A, submitted

Duschl, W. J., & Lesch, H. 1994, A&A, 286, 431

Eckart, A., & Genzel, R. 1996, Nature, 383, 415

Eckart, A., & Genzel, R. 1997, MNRAS, 284, 576

Eckart, A., Genzel, R., Hofmann, R., Sams, B. J., & Tacconi-Garman, L. E. 1993, ApJ, 407, L77

Eckart, A., Genzel, R., Hofmann, R., Sams, B. J., & Tacconi-Garman, L. E. 1995, ApJ, 445, L23

Eckart, A., Genzel, R., Krabbe, A., Hofmann, R., van Der Werf, P. P., & Drapatz, S. 1992, Nature, 355, 526

Ekers, R. D., Goss, W. M., Schwarz, U. J., Downes, D., & Rogstad, D. H. 1975, A&A, 43, 159

Ekers, R. D., van Gorkom, J. H., Schwarz, U. J., & Goss, W. M. 1983, A&A, 122, 143

Falcke, H. 1996a, ApJ, 464, L67

Falcke, H. 1996b, in IAU Symp. 169: Unsolved Problems of the Milky Way, ed. L. Blitz & P. Teuben, Vol. 169 (Dordrecht: Kluwer), 169

Falcke, H. 1999, in ASP Conf. Ser. 186: The Central Parsecs of the Galaxy, ed. H. Falcke, A. Cotera, W. Duschl, F. Melia, & M. J. Rieke (San Francisco: Astronomical Society of the Pacific), 113

Falcke, H., & Biermann, P. L. 1995, A&A, 293, 665

Falcke, H., & Biermann, P. L. 1999, A&A, 342, 49

Falcke, H., Goss, W. M., Matsuo, H., Teuben, P., Zhao, J. H., & Zylka, R. 1998, ApJ, 499, 731

Falcke, H., Mannheim, K., & Biermann, P. L. 1993, A&A, 278, L1

Falcke, H., & Markoff, S. 2000, A&A, 362, 113

Falcke, H., & Melia, F. 1997, ApJ, 479, 740

Falcke, H., Melia, F., & Agol, E. 2000, ApJ, 528, L13

Falcke, H., Nagar, N. M., Wilson, A. S., & Ulvestad, J. S. 2000, ApJ, 542, 197

Fatuzzo, M., Melia, F., & Rafelski, J. 2001, ApJ, 549, 293

Figer, D. F., Kim, S. S., Morris, M., Serabyn, E., Rich, R. M., & McLean, I. S. 1999a, ApJ, 525, 750

Figer, D. F., Morris, M., Geballe, T. R., Rich, R. M., Serabyn, E., McLean, I. S., Puetter, R. C., & Yahil, A. 1999b, ApJ, 525, 759

Fromerth, M. J., & Melia, F. 2001, ApJ, 549, 205

Genzel, R., & Eckart, A. 1999, in ASP Conf. Ser. 186: The Central Parsecs of the Galaxy, ed. H. Falcke, A. Cotera, W. Duschl, F. Melia, & M. J. Rieke (San Francisco: Astronomical Society of the Pacific), 3

Genzel, R., Eckart, A., Ott, T., & Eisenhauer, F. 1997, MNRAS, 291, 219

Genzel, R., Thatte, N., Krabbe, A., Kroker, H., & Tacconi-Garman, L. E. 1996, ApJ, 472, 153

Genzel, R., & Townes, C. H. 1987, ARA&A, 25, 377

Gezari, D. 1996, in ASP Conf. Ser., Vol. 102, The Galactic Center, ed. R. Gredel (San Francisco: Astronomical Society of the Pacific), 491

Ghez, A. M., Klein, B. L., Morris, M., & Becklin, E. E. 1998, ApJ, 509, 678

Ghez, A. M., Morris, M., & Becklin, E. E. 1999, in ASP Conf. Ser. 186: The Central Parsecs of the Galaxy, ed. H. Falcke, A. Cotera, W. Duschl, F. Melia, & M. J. Rieke (San Francisco: Astronomical Society of the Pacific), 18

Ghez, A. M., Morris, M., & Becklin, E. E. 2000, International Conference of the Astronomische Gesellschaft at Heidelberg, March 20-24, 2000, 16, 28

Ghez, A. M., Morris, M., Becklin, E. E., Tanner, A., & Kremenek, T. 2000, Nature, 407, 349

Goldwurm, A., et al. 1994, Nature, 371, 589

Gray, A. D., Cram, L. E., Ekers, R. D., & Goss, W. M. 1991, Nature, 353, 237

Gwinn, C. R., Danen, R. M., Tran, T. K., Middleditch, J., & Ozernoy, L. M. 1991, ApJ, 381, L43

Haller, J. W., & Melia, F. 1996, ApJ, 464, 774

Haller, J. W., Rieke, M. J., Rieke, G. H., Tamblyn, P., Close, L., & Melia, F. 1996, ApJ, 456, 194

Hayashida, N., et al. 1999, Astroparticle Physics, 10, 303

Herbst, T. M., Beckwith, S. V. W., Forrest, W. J., & Pipher, J. L. 1993, AJ, 105, 956

Ho, L. C., Filippenko, A. V., & Sargent, W. L. W. 1997, ApJS, 112, 315

Hughes, P. A., Aller, H. D., & Aller, M. F. 1985, ApJ, 298, 301

Hujeirat, A. 1999, AG Abstract Services, vol. 15. Abstracts of Contributed Talks and Posters presented at the Annual Scientific Meeting of the Astronomische Gesellschaft, in Goettingen, 20-25 September 1999., 15, 10

Igumenshchev, I. V., Abramowicz, M. A., & Narayan, R. 2000, ApJ, 537, L27

Igumenshchev, I. V., Chen, X., & Abramowicz, M. A. 1996, MNRAS, 278, 236

Ipser, J. R., & Price, R. H. 1982, ApJ, 255, 654

Jackson, J. M., Geis, N., Genzel, R., Harris, A. I., Madden, S., Poglitsch, A., Stacey, G. J., & Townes, C. H. 1993, ApJ, 402, 173

Kassim, N. E., Larosa, T. N., Lazio, T. J. W., & Hyman, S. D. 1999, in ASP Conf. Ser. 186: The Central Parsecs of the Galaxy, ed. H. Falcke, A. Cotera, W. Duschl, F. Melia, & M. J. Rieke (San Francisco: Astronomical Society of the Pacific), 403

Kellermann, K. I., & Pauliny-Toth, I. I. K. 1969, ApJ, 155, L71

Khokhlov, A., & Melia, F. 1996, ApJ, 457, L61

Killeen, N. E. B., Lo, K. Y., & Crutcher, R. 1992, ApJ, 385, 585

Kino, M., Kaburaki, O., & Yamazaki, N. 2000, ApJ, 536, 788

Koide, S., Meier, D. L., Shibata, K., & Kudoh, T. 2000, ApJ, 536, 668

Kowalenko, V., & Melia, F. 1999, MNRAS, 310, 1053

Koyama, K., Maeda, Y., Sonobe, T., Takeshima, T., Tanaka, Y., & Yamauchi, S. 1996, PASJ, 48, 249

Krabbe, A., et al. 1995, ApJ, 447, L95

Krichbaum, T. P., Graham, D. A., Witzel, A., Greve, A., Wink, J. E., Grewing, M., Colomer, F., de Vicente, P., Gomez-Gonzalez, J., Baudry, A., & Zensus, J. A. 1998, A&A, 335, L106

Krichbaum, T. P., Witzel, A., & Zensus, J. A. 1999, in ASP Conf. Ser. 186: The Central Parsecs of the Galaxy, ed. H. Falcke, A. Cotera, W. Duschl, F. Melia, & M. J. Rieke (San Francisco: Astronomical Society of the Pacific), 89

Krichbaum, T. P., et al. 1993, A&A, 274, L37

Kundt, W. 1990, Ap&SS, 172, 109

Lacy, J. H., Townes, C. H., Geballe, T. R., & Hollenbach, D. J. 1980, ApJ, 241, 132

Lang, C. C., Morris, M., & Echevarria, L. 1999, ApJ, 526, 727

LaRosa, T. N., Kassim, N. E., Lazio, T. J. W., & Hyman, S. D. 2000, AJ, 119, 207

Latvakoski, H. M., Stacey, G. J., Gull, G. E., & Hayward, T. L. 1999, ApJ, 511, 761

Liszt, H. S. 1985, ApJ, 293, L65

Lo, K. Y., Backer, D. C., Kellermann, K. I., Reid, M., Zhao, J. H., Goss, W. M., & Moran, J. M. 1993, Nature, 362, 38

Lo, K. Y., & Claussen, M. J. 1983, Nature, 306, 647

Lo, K. Y., Schilizzi, R. T., Cohen, M. H., & Ross, H. N. 1975, ApJ, 202, L63

Lo, K. Y., Shen, Z. Q., Zhao, J. H., & Ho, P. T. P. 1998, ApJ, 508, L61

Lynden-Bell, D., & Rees, M. J. 1971, MNRAS, 152, 461

Maeda, Y., Baganoff, F. K., Feigelson, E. D., Morris, M., Bautz, M. W., Brandt, W. N., Burrows, D. N., Doty, J. P., Garmire, G. P., Pravdo, S. H., Ricker, G. R., & Townsley, L. K. 2001, ApJ, submitted

Mahadevan, R. 1999, MNRAS, 304, 501

Mahadevan, R., Narayan, R., & Yi, I. 1996, ApJ, 465, 327

Manmoto, T. 2000, ApJ, 534, 734

Manmoto, T., Kato, S., Nakamura, K. E., & Narayan, R. 2000, ApJ, 529, 127

Maoz, E. 1998, ApJ, 494, L181

Marcaide, J. M., Alberdi, A., Lara, L., Pérez-Torres, M. A., & Diamond, P. J. 1999, A&A, 343, 801

Markoff, S., Falcke, H., & Biermann, P. L. 2000, in preparation

Markoff, S., Melia, F., & Sarcevic, I. 1997, ApJ, 489, L47

Markoff, S., Melia, F., & Sarcevic, I. 1999, ApJ, 522, 870

Marscher, A. P., & Gear, W. K. 1985, ApJ, 298, 114

Mathis, J. S. 1990, ARA&A, 28, 37

Mayer-Hasselwander, H. A., et al. 1998, A&A, 335, 161

Melia, F. 1992, ApJ, 387, L25

Melia, F. 1994, ApJ, 426, 577

Melia, F., Bromley, B. C., Liu, S., & Walker, C. K. 2001, ApJ, in press

Melia, F., & Coker, R. 1999, ApJ, 511, 750

Melia, F., Coker, R. F., & Yusef-Zadeh, F. 1996, ApJ, 460, L33

Melia, F., Jokipii, J. R., & Narayanan, A. 1992, ApJ, 395, L87

Melia, F., Liu, S., & Coker, R. 2000, ApJ, 545, L117

Melia, F., Liu, S., & Coker, R. 2001, ApJ, in press

Menou, K., Quataert, E., & Narayan, R. 1999, in Recent Developments in Theoretical and Experimental General Relativity, Gravitation, and Relativistic Field Theories, ed. T. Piran & R. Ruffini (World Scientific Publishers), 204

Menten, K. M., Reid, M. J., Eckart, A., & Genzel, R. 1997, ApJ, 475, L111

Mezger, P. G., Duschl, W. J., & Zylka, R. 1996, A&A Rev., 7, 289

Mezger, P. G., Zylka, R., Salter, C. J., Wink, J. E., Chini, R., Kreysa, E., & Tuffs, R. 1989, A&A, 209, 337

Morris, M. 1994, in Normal Galactic Nuclei: Lessons from the Galactic Center, ed. R. Genzel & A. I. Harris (Dordrecht: Kluwer), 185

Morris, M., Ghez, A. M., & Becklin, E. E. 1999, Advances in Space Research, 23, 959

Morris, M., & Serabyn, E. 1996, ARA&A, 34, 645

Munyaneza, F., Tsiklauri, D., & Viollier, R. D. 1999, ApJ, 526, 744

Nagar, N. M., Falcke, H., Wilson, A. S., & Ho, L. C. 2000, ApJ, 542, 186

Najarro, F., Hillier, D. J., Kudritzki, R. P., Krabbe, A., Genzel, R., Lutz, D., Drapatz, S., & Geballe, T. R. 1994, A&A, 285, 573

Najarro, F., Krabbe, A., Genzel, R., Lutz, D., Kudritzki, R. P., & Hillier, D. J. 1997, A&A, 325, 700

Narayan, R., Igumenshchev, I. V., & Abramowicz, M. A. 2000, ApJ, 539, 798

Narayan, R., Mahadevan, R., Grindlay, J. E., Popham, R. G., & Gammie, C. 1998, ApJ, 492, 554

Narayan, R., & Yi, I. 1994, ApJ, 428, L13

Narayan, R., Yi, I., & Mahadevan, R. 1995, Nature, 374, 623

Novak, G. 1999, in ASP Conf. Ser. 186: The Central Parsecs of the Galaxy, ed. H. Falcke, A. Cotera, W. Duschl, F. Melia, & M. J. Rieke (San Francisco: Astronomical Society of the Pacific), 488

Novak, G., Dotson, J. L., Dowell, C. D., Hildebrand, R. H., Renbarger, T., & Schleuning, D. A. 2000, ApJ, 529, 241

Osterbrock, D. E. 1989, in Astrophysics of Gaseous Nebulae and Active Galactic Nuclei (Mill Valley, CA: University Science Books)

Pedlar, A., Anantharamaiah, K. R., Ekers, R. D., Goss, W. M., van Gorkom, J. H., Schwarz, U. J., & Zhao, J. 1989, ApJ, 342, 769

Peterson, B. M. 1997, in An Introduction to Active Galactic Nuclei (Cambridge: Cambridge University Press)

Petschek, H. E. 1998, Ap&SS, 264, 9

Plante, R. L., Lo, K. Y., & Crutcher, R. M. 1995, ApJ, 445, L113

Predehl, P., & Trümper, J. 1994, A&A, 290, L29

Predehl, P., & Zinnecker, H. 1996, in ASP Conf. Ser., Vol. 102, The Galactic Center, ed. R. Gredel (San Francisco: Astronomical Society of the Pacific), 415

Quataert, E., & Gruzinov, A. 2000a, ApJ, 545, 842

Quataert, E., & Gruzinov, A. 2000b, ApJ, 539, 809

Quataert, E., Narayan, R., & Reid, M. J. 1999, ApJ, 517, 101

Rantakyro, F. T., et al. 1998, A&AS, 131, 451

Readhead, A. C. S. 1994, ApJ, 426, 51

Rees, M. J. 1982, in AIP Conf. Proc. 83: The Galactic Center, ed. G. R. Riegler & R. D. Blandford (New York: American Institute of Physics), 166

Reich, W., Sofue, Y., & Matsuo, H. 2000, PASJ, 52, 355

Reid, M. J. 1993, ARA&A, 31, 345

Reid, M. J., Readhead, A. C. S., Vermeulen, R. C., & Treuhaft, R. N. 1999, ApJ, 524, 816

Reynolds, S. P., & McKee, C. F. 1980, ApJ, 239, 893

Rieke, G. H., & Lebofsky, M. J. 1982, in AIP Conf. Proc. 83: The Galactic Center, 194

Rieke, G. H., & Lebofsky, M. J. 1985, ApJ, 288, 618

Rieke, G. H., & Rieke, M. J. 1988, ApJ, 330, L33

Roberts, D. A. 1999, in ASP Conf. Ser. 186: The Central Parsecs of the Galaxy, ed. H. Falcke, A. Cotera, W. Duschl, F. Melia, & M. J. Rieke (San Francisco: Astronomical Society of the Pacific), 483

Roberts, D. A., Yusef-Zadeh, F., & Goss, W. M. 1996, ApJ, 459, 627

Rogers, A. E. E., Doeleman, S., Wright, M. C. H., Bower, G. C., Backer, D. C., Padin, S., Philips, J. A., Emerson, D. T., Greenhill, L., Moran, J. M., & Kellermann, K. I. 1994, ApJ, 434, L59

Romani, R. W., Narayan, R., & Blandford, R. 1986, MNRAS, 220, 19

Rosa, M. R., Zinnecker, H., Moneti, A., & Melnick, J. 1992, A&A, 257, 515

Salim, S., & Gould, A. 1999, ApJ, 523, 633

Sanders, R. H. 1999, in ASP Conf. Ser. 186: The Central Parsecs of the Galaxy, ed. H. Falcke, A. Cotera, W. Duschl, F. Melia, & M. J. Rieke (San Francisco: Astronomical Society of the Pacific), 250

Sault, R. J., & Macquart, J. P. 1999, ApJ, 526, L85

Sellgren, K., McGinn, M. T., Becklin, E. E., & Hall, D. N. 1990, ApJ, 359, 112

Serabyn, E., Carlstrom, J., Lay, O., Lis, D. C., Hunter, T. R., & Lacy, J. H. 1997, ApJ, 490, L77

Serabyn, E., & Lacy, J. H. 1985, ApJ, 293, 445

Serabyn, E., Lacy, J. H., Townes, C. H., & Bharat, R. 1988, ApJ, 326, 171

Serabyn, E., & Morris, M. 1994, ApJ, 424, L91

Shapiro, S. L. 1973, ApJ, 180, 531

Shields, J. C., & Ferland, G. J. 1994, ApJ, 430, 236

Sidoli, L., & Mereghetti, S. 1999, A&A, 349, L49

Sofue, Y., & Lang, C. C. 1999, in ASP Conf. Ser. 186: The Central Parsecs of the Galaxy, ed. H. Falcke, A. Cotera, W. Duschl, F. Melia, & M. J. Rieke (San Francisco: Astronomical Society of the Pacific), 519

Stolovy, S. R., Hayward, T. L., & Herter, T. 1996, ApJ, 470, L45

Stolovy, S. R., McCarthy, D. W., Melia, F., Rieke, G., Rieke, M. J., & Yusef-Zadeh, F. 1999, in ASP Conf. Ser. 186: The Central Parsecs of the Galaxy, ed. H. Falcke, A. Cotera, W. Duschl, F. Melia, & M. J. Rieke (San Francisco: Astronomical Society of the Pacific), 39

Tamblyn, P., & Rieke, G. H. 1993, ApJ, 414, 573

Tanner, A. M., Ghez, A. M., Morris, M., & Becklin, E. E. 1999, in ASP Conf. Ser. 186: The Central Parsecs of the Galaxy, ed. H. Falcke, A. Cotera, W. Duschl, F. Melia, & M. J. Rieke (San Francisco: Astronomical Society of the Pacific), 351

Telesco, C. M., Davidson, J. A., & Werner, M. W. 1996, ApJ, 456, 541

Torres, D. F., Capozziello, S., & Lambiase, G. 2000, Phys. Rev. D, 62, 104012

Townes, C. H. 1996, in IAU Symp. 169: Unsolved Problems of the Milky Way, Vol. 169, 149

Tsiklauri, D., & Viollier, R. D. 1998, ApJ, 500, 591

Tsuboi, M., Miyazaki, A., & Tsutsumi, T. 1999, in ASP Conf. Ser. 186: The Central Parsecs of the Galaxy, ed. H. Falcke, A. Cotera, W. Duschl, F. Melia, & M. J. Rieke (San Francisco: Astronomical Society of the Pacific), 105

Turolla, R., & Dullemond, C. P. 2000, ApJ, 531, L49

van Hoven, G., Hendrix, D. L., & Schnack, D. D. 1995, J. Geophys. Res., 100, 19819

van Langevelde, H. J., Frail, D. A., Cordes, J. M., & Diamond, P. J. 1992, ApJ, 396, 686

von Linden, S., Biermann, P. L., Duschl, W. J., Lesch, H., & Schmutzler, T. 1993, A&A, 280, 468

Weiler, K. W., & de Pater, I. 1983, ApJS, 52, 293

Wilson, A. S. 2000, in Darwin and Astronomy: The Infrared Space Interferometer (European Space Agency ESA SP-451), 91

Wright, M. C. H., & Backer, D. C. 1993, ApJ, 417, 560

Wrobel, J. M., & Heeschen, D. S. 1984, ApJ, 287, 41

Yuan, F. 2000, MNRAS, 319, 1178

Yuan, F., Peng, Q., Lu, J., & Wang, J. 2000, ApJ, 537, 236

Yusef-Zadeh, F., Cotton, W., Wardle, M., Melia, F., & Roberts, D. A. 1994, ApJ, 434, L63

Yusef-Zadeh, F., Melia, F., & Wardle, M. 2000, Science, 287, 95

Yusef-Zadeh, F., & Morris, M. 1987, ApJ, 320, 545

Yusef-Zadeh, F., Morris, M., & Chance, D. 1984, Nature, 310, 557

Yusef-Zadeh, F., Roberts, D. A., & Biretta, J. 1998, ApJ, 499, L159

Yusef-Zadeh, F., Stolovy, S. R., Burton, M., Wardle, M., Melia, F., Lazio, T. J. W., Kassim, N. E., & Roberts, D. A. 1999, in ASP Conf. Ser. 186: The Central Parsecs of the Galaxy, ed. H. Falcke, A. Cotera, W. Duschl, F. Melia, & M. J. Rieke (San Francisco: Astronomical Society of the Pacific), 197

Yusef-Zadeh, F., & Wardle, M. 1993, ApJ, 405, 584

Zensus, J. A. 1997, ARA&A, 35, 607

Zhao, J., Bower, G. C., & Goss, W. M. 2001, ApJ, 547, L29

Zhao, J., Ekers, R. D., Goss, W. M., Lo, K. Y., & Narayan, R. 1989, in IAU Symp. 136: The Center of the Galaxy, ed. M. Morris, Vol. 136 (Dordrecht: Kluwer), 535

Zhao, J., & Goss, W. M. 1998, ApJ, 499, L163

Zhao, J. H., & Goss, W. M. 1999, in ASP Conf. Ser. 186: The Central Parsecs of the Galaxy, ed. H. Falcke, A. Cotera, W. Duschl, F. Melia, & M. J. Rieke (San Francisco: Astronomical Society of the Pacific), 224

Zhao, J. H., Goss, W. M., Lo, K. Y., & Ekers, R. D. 1992, in ASP Conf. Ser. 31: Relationships Between Active Galactic Nuclei and Starburst Galaxies, ed. A. V. Filippenko (San Francisco: ASP), 295

Zylka, R., Güsten, R., Philipp, S., Ungerechts, H., Mezger, P. G., & Duschl, W. J. 1999, in ASP Conf. Ser. 186: The Central Parsecs of the Galaxy, ed. H. Falcke, A. Cotera, W. Duschl, F. Melia, & M. J. Rieke (San Francisco: Astronomical Society of the Pacific), 415

Zylka, R., Mezger, P. G., & Lesch, H. 1992, A&A, 261, 119

Zylka, R., Mezger, P. G., Ward-Thompson, D., Duschl, W. J., & Lesch, H. 1995, A&A, 297, 83